

# Structure–Function Relationships in Yeast Tubulins<sup>□</sup>

Kristy L. Richards,<sup>\*†</sup> Kirk R. Anders,<sup>\*†</sup> Eva Nogales,<sup>‡§</sup> Katja Schwartz,<sup>\*</sup>  
Kenneth H. Downing,<sup>§</sup> and David Botstein<sup>\*||</sup>

<sup>\*</sup>Department of Genetics, Stanford University School of Medicine, Stanford, California 94305;

<sup>‡</sup>Department of Molecular and Cell Biology, University of California at Berkeley, Berkeley, California 94720; and <sup>§</sup>Lawrence Berkeley National Laboratory, Berkeley, California 94720

Submitted December 15, 1999; Revised February 28, 2000; Accepted March 3, 2000

Monitoring Editor: David Drubin

A comprehensive set of clustered charged-to-alanine mutations was generated that systematically alter *TUB1*, the major  $\alpha$ -tubulin gene of *Saccharomyces cerevisiae*. A variety of phenotypes were observed, including supersensitivity and resistance to the microtubule-destabilizing drug benomyl, lethality, and cold- and temperature-sensitive lethality. Many of the most benomyl-sensitive *tub1* alleles were synthetically lethal in combination with *tub3* $\Delta$ , supporting the idea that benomyl supersensitivity is a rough measure of microtubule instability and/or insufficiency in the amount of  $\alpha$ -tubulin. The systematic *tub1* mutations were placed, along with the comparable set of *tub2* mutations previously described, onto a model of the yeast  $\alpha$ - $\beta$ -tubulin dimer based on the three-dimensional structure of bovine tubulin. The modeling revealed a potential site for binding of benomyl in the core of  $\beta$ -tubulin. Residues whose mutation causes cold sensitivity were concentrated at the lateral and longitudinal interfaces between adjacent subunits. Residues that affect binding of the microtubule-binding protein Bim1p form a large patch across the exterior-facing surface of  $\alpha$ -tubulin in the model. Finally, the positions of the mutations suggest that proximity to the  $\alpha$ - $\beta$  interface may account for the finding of synthetic lethality of five viable *tub1* alleles with the benomyl-resistant but otherwise entirely viable *tub2-201* allele.

## INTRODUCTION

Microtubules are ubiquitous cytoskeletal structures, made up of heterodimers of  $\alpha$  and  $\beta$ -tubulin (Hyams and Lloyd, 1994). Microtubules have been studied in many eukaryotes, both in vitro and in vivo, with the aim of defining both the functions of microtubules and the spatial and temporal regulation of those microtubule functions. As in all eukaryotic cells, microtubules are necessary for chromosome movement in *Saccharomyces cerevisiae*. Unlike most other eukaryotes, the only other functions known to depend on microtubules in yeast are the movement of nuclei to the bud neck before mitosis and the fusion of nuclei after mating (Huffaker *et al.*, 1988; Jacobs *et al.*, 1988). The high degree of conservation among tubulin proteins (Little and Seehaus, 1988; Burns, 1991), together with the relative simplicity of the yeast microtubule cytoskeleton, make *S. cerevisiae* a suitable organism for studying the microtubule cytoskeleton.

*TUB1* is the major gene encoding  $\alpha$ -tubulin in *S. cerevisiae* (Schatz *et al.*, 1986a,b), and *TUB2* is the only gene encoding

the  $\beta$ -tubulin gene (Neff *et al.*, 1983). *TUB3* is a second gene encoding  $\alpha$ -tubulin; it is expressed at lower levels than *TUB1* (Schatz *et al.*, 1986a,b). *TUB1* and *TUB2* are essential genes, whereas a strain carrying a deletion of *TUB3* is viable. *tub3* null mutations, and most *tub1* mutations, show a characteristic supersensitivity to the benzimidazole microtubule drug benomyl (Neff *et al.*, 1983; Schatz *et al.*, 1986b). Deletion of *TUB1* produces a dominant phenotype resulting from haploinsufficiency; heterozygotes tend to become trisomic for the wild-type chromosome XIII, which presumably provides a growth advantage because of an additional copy of both *TUB1* and *TUB3* (Schatz *et al.*, 1986b). The two genes encoding  $\alpha$ -tubulin in yeast are very similar, producing protein products that are ~90% identical, making them much more similar to each other than to  $\alpha$ -tubulin proteins from other organisms, to which they are ~70% identical (Little and Seehaus, 1988). Either  $\alpha$ -tubulin gene, *TUB1* or *TUB3*, can compensate for loss of the other, if expressed at high enough levels. Therefore, the differences between *TUB1* and *TUB3* appear to be largely quantitative, resulting from higher levels of *TUB1* expression, rather than qualitative (i.e., sequence) differences in the proteins (Schatz *et al.*, 1986b).

Clustered charged-to-alanine scanning mutagenesis has been used to mutagenize the surface of proteins systematically (Bass *et al.*, 1991; Bennett *et al.*, 1991; Gibbs and Zoller, 1991). This strategy has been used previously to mutagenize

<sup>□</sup> A complete data set for this article is available at [www.molbiolcell.org](http://www.molbiolcell.org).

<sup>†</sup> These authors contributed equally to this work.

<sup>||</sup> Corresponding author. E-mail address: [botstein@genome.stanford.edu](mailto:botstein@genome.stanford.edu).

**Table 1.** Plasmids used in this study

Plasmid	Description	Source or reference
pUC119	pUC19 with M13 origin of replication	Sambrook <i>et al.</i> , 1989
pRB306	<i>TUB1</i> in pRB322	Schatz <i>et al.</i> , 1986b
pRB326	<i>TUB1</i> in YCp50	Schatz <i>et al.</i> , 1986b
pJJ217	<i>HIS3</i> in pUC18 polylinker	Jones and Prakash, 1990
pJJ282	<i>LEU2</i> in pUC18 polylinker	Jones and Prakash, 1990
pRS317	<i>LYS2</i> in pRSS56	Sikorski and Hieter, 1989
pRB2063	<i>TUB1</i> fragment ( <i>SphI</i> – <i>SacI</i> ) from pRB306 inserted into <i>SphI</i> – <i>SacI</i> -cut polylinker of pUC119	This study
pRB2065	<i>BamHI</i> – <i>SallI</i> fragment from pJJ282 ( <i>LEU2</i> gene) Klenow filled and inserted into the <i>HpaI</i> site of pRB2063, downstream of <i>TUB1</i> ; <i>LEU2</i> is oriented in the same direction as <i>TUB1</i>	This study
pRB2067	<i>SallI</i> – <i>KpnI</i> (partial) fragment from pJJ217 containing the entire <i>HIS3</i> gene and flanking regions, inserted into <i>XhoI</i> – <i>KpnI</i> vector fragment from pRB2063; <i>HIS3</i> is in the same orientation that <i>TUB1</i> was; note that this disruption construct removes the first 763 bp of the 1580-bp ORF downstream of <i>TUB1</i> (YML086c)	This study
pRB2070	<i>PvuII</i> fragment from pRS317 containing <i>LYS2</i> gene inserted into <i>HpaI</i> site of pRB2063; <i>LYS2</i> is oriented in the same direction as <i>TUB1</i>	This study
pRB2666	<i>BglIII</i> fragment containing <i>TUB3</i> from pRB300 ligated into <i>BamHI</i> site of pUC119	This study
pRB2668	<i>SallI</i> – <i>SmaI</i> containing <i>HIS3</i> fragment from pJJ217 ligated into <i>XhoI</i> – <i>NdeI</i> (Klenow-filled) vector fragment from pRB2666; <i>HIS3</i> is in the same orientation as <i>TUB3</i> was	This study
pRB2254 through pRB2412	pRB2065 mutagenized via site-directed mutagenesis, yielding three isolates of each Ala-scan mutation, <i>tub1-801</i> through <i>tub1-853</i>	This study

the two other major cytoskeletal proteins in *S. cerevisiae*, actin and  $\beta$ -tubulin (Wertman *et al.*, 1992; Reijo *et al.*, 1994). In the case of *ACT1* (the single yeast gene encoding actin), such a program of mutagenesis produced many conditionally lethal alleles, which had previously proven quite difficult to isolate (Wertman *et al.*, 1992). In the case of *TUB2* (the sole  $\beta$ -tubulin gene), many new conditional alleles were obtained, some displaying previously unreported phenotypes (Reijo *et al.*, 1994). Both of these sets of mutants are proving to be useful in studies of the cytoskeleton in yeast (Pasqualone and Huffaker, 1994; Amberg *et al.*, 1995; Cali *et al.*, 1998).

Recently the structure of bovine tubulin has been solved at atomic resolution (Nogales *et al.*, 1998b). This allows the results of years of study of the tubulin genes and the function of microtubules in yeast to be analyzed in light of the three-dimensional structure of the tubulin protein. In this paper we map nearly all the known systematic mutations in *TUB1* and *TUB2* to a model of yeast tubulin based on the bovine structure. As had been found with actin and cofilin (Wertman *et al.*, 1992; Lappalainen *et al.*, 1997), this mapping has indicated regions of the tubulin surface implicated in particular phenotypes, namely cold sensitivity and benomyl resistance. In addition, we have found evidence for the involvement of particular residues in binding of the microtubule ligand Bim1p (Schwartz *et al.*, 1997), and others have found similar evidence for other proteins that bind tubulins (Feierbach *et al.*, 1999).

## MATERIALS AND METHODS

### Media and Genetic Manipulations

Yeast media and techniques are as described (Rose *et al.*, 1990), except that YPD medium was supplemented with adenine sulfate to

a concentration of 40 mg/l. Minimal medium was supplemented only with the required amino acids, rather than using synthetic complete medium, unless specified. Permissive temperature for all experiments was 25°C. Sporulation was induced by diluting a liquid culture 100-fold into sporulation medium described by Kassir and Simchen (1991). Benomyl, a generous gift from DuPont (Wilmington, DE), was kept as a 10 mg/ml stock in dimethylsulfoxide at –20°C. It was added to warm medium, with vigorous swirling to prevent precipitation of the benomyl, just before pouring plates. Bacterial media and techniques were as described (Sambrook *et al.*, 1989). Ampicillin was used at a final concentration of 50  $\mu$ g/ml.

### Strains and Plasmids

Plasmids are listed in Table 1, along with details of their construction. Yeast strains were derived from YPH102 and YPH250 (Sikorski and Hieter, 1989) and are listed in Table 2. YPH102 was transformed with a *TUB1* CEN plasmid, pRB326. The resulting strain, KRY73, was transformed with a *tub1* deletion construct from pRB2067, to give DBY6590. DBY6591 was constructed by transforming YPH250 with the *TUB1*–*LYS2* construct from pRB2070. DBY6590 was crossed to DBY6591 to give the diploid KRY76. KRY76 was dissected to remove the *trp1*– $\Delta 1$  allele, and two resulting spores, DBY6592 and DBY6593, were crossed, yielding DBY6596. DBY6596 was the recipient strain for the Ala-scan alleles, and its genomic configuration was verified by Southern blot analysis. Mating type tester strains DBY786 and DBY789 were essentially congenic with S288C. Bacterial strains used for transformation and propagation of plasmid DNA were either DH5 $\alpha$  or DH5 $\alpha$ F' (Sambrook *et al.*, 1989).

To construct the *tub3* $\Delta$  strain, DBY6592 was transformed with the gel-purified 2.8-kb *BstEII*–*HindIII* fragment from pRB2668, obtained from a *BstEII* digest followed by a partial *HindIII* digest, to give DBY6598. The proper genomic organization of the strain was verified by Southern blot analysis. To obtain a congenic strain of the opposite mating type, DBY6598 was mated to DBY6654, yielding the haploid His<sup>+</sup> Lys<sup>+</sup> Ura<sup>+</sup> segregant DBY6599.

**Table 2.** Yeast strains used in this study

Strain	Genotype	Source or reference
YPH102	<i>MAT<math>\alpha</math></i> <i>ade2-101 his3-<math>\Delta</math>200 lys2-801 leu2-<math>\Delta</math>1 ura3-52</i>	Sikorski and Hieter, 1989
YPH250	<i>MATa</i> <i>ade2-101 his3-<math>\Delta</math>200 lys2-801 leu2-<math>\Delta</math>1 ura3-52 trp1-<math>\Delta</math>1</i>	Sikorski and Hieter, 1989
DBY786	<i>MAT<math>\alpha</math></i> <i>trp1-1</i>	This laboratory
DBY789	<i>MATa</i> <i>trp1-1</i>	This laboratory
KRY73	<i>MAT<math>\alpha</math></i> <i>ade2-101 his3-<math>\Delta</math>200 lys2-801 leu2-<math>\Delta</math>1 ura3-52</i> plasmid: pRB326	This study
DBY6590	<i>MAT<math>\alpha</math></i> <i>ade2-101 his3-<math>\Delta</math>200 lys2-801 leu2-<math>\Delta</math>1 ura3-52 tub1<math>\Delta</math>::HIS3</i> plasmid: pRB326	This study
DBY6591	<i>MATa</i> <i>ade2-101 his3-<math>\Delta</math>200 lys2-801 leu2-<math>\Delta</math>1 ura3-52 trp1-<math>\Delta</math>1 TUB1-LYS2</i>	This study
KRY76 (DBY6590 × 6591)	<i>MATa<math>\alpha</math></i> <i>ade2-101/ade2-101 his3-<math>\Delta</math>200/his3-<math>\Delta</math>200 lys2-801/lys2-801 leu2-<math>\Delta</math>1/leu2-<math>\Delta</math>1 ura3-52/ura3-52 trp1-<math>\Delta</math>1/TRP1 TUB1-LYS2/tub1<math>\Delta</math>::HIS3</i> plasmid: pRB326	This study
DBY6592	<i>MAT<math>\alpha</math></i> <i>lys2-801 ade2-101 his3-<math>\Delta</math>200 leu2-<math>\Delta</math>1 ura3-52 TUB1-LYS2</i> plasmid: pRB326	This study
DBY6593	<i>MATa</i> <i>lys2-801 ade2-101 his3-<math>\Delta</math>200 leu2-<math>\Delta</math>1 ura3-52 tub1<math>\Delta</math>::HIS3</i> plasmid: pRB326	This study
DBY6596	<i>MATa<math>\alpha</math></i> <i>lys2-801/lys2-801 ade2-101/ade2-101 his3-<math>\Delta</math>200/his3-<math>\Delta</math>200 leu2-<math>\Delta</math>1/leu2-<math>\Delta</math>1 ura3-52/ura3-52 TUB1-LYS2/tub1<math>\Delta</math>::HIS3</i> plasmid: pRB326	This study
DBY6598	<i>MAT<math>\alpha</math></i> <i>lys2-801 ade2-101 his3-<math>\Delta</math>200 leu2-<math>\Delta</math>1 ura3-52 TUB1-LYS2 tub3<math>\Delta</math>::HIS3</i> plasmid: pRB326	This study
DBY6599	<i>MATa</i> <i>lys2-801 ade2-101 his3-<math>\Delta</math>200 leu2-<math>\Delta</math>1 ura3-52 TUB1-LYS2 tub3<math>\Delta</math>::HIS3</i> plasmid: pRB326	This study
DBY6600	<i>MATa<math>\alpha</math></i> <i>lys2-801/lys2-801 ade2-101/ade2-101 his3-<math>\Delta</math>200/his3-<math>\Delta</math>200 leu2-<math>\Delta</math>1/leu2-<math>\Delta</math>1 ura3-52/ura3-52 TUB1-LYS2/TUB1-LEU2</i> plasmid pRB326	This study
DBY6601–6653	Like DBY6600, but with <i>tub1</i> Ala-scan alleles, -801 to -853, respectively	This study
DBY6654	<i>MATa</i> <i>lys2-801 ade2-101 his3-<math>\Delta</math>200 leu2-<math>\Delta</math>1 ura3-52 TUB1-LEU2</i>	This study
DBY6655	<i>MAT<math>\alpha</math></i> <i>lys2-801 ade2-101 his3-<math>\Delta</math>200 leu2-<math>\Delta</math>1 ura3-52 TUB1-LEU2</i>	This study
DBY6656–6761	Like DBY6654 and 6655, but with <i>tub1</i> Ala-scan alleles, -801 to -853, respectively (2 each, 1 of each mating type)	This study
DBY6762	<i>MATa<math>\alpha</math></i> <i>lys2-801/lys2-801 ade2-101/ade2-101 his3-<math>\Delta</math>200/his3-<math>\Delta</math>200 leu2-<math>\Delta</math>1/leu2-<math>\Delta</math>1 ura3-52/ura3-52 TUB1-LYS2/TUB1-LEU2 tub3<math>\Delta</math>::HIS3/TUB3</i> plasmid: pRB326	This study
DBY6816	<i>MATa</i> <i>lys2-801 ade2-101 his3-<math>\Delta</math>200 leu2-<math>\Delta</math>1 ura3-52 TUB1-LEU2 tub3<math>\Delta</math>::HIS3</i>	This study
DBY6822	<i>MATa</i> <i>lys2-801 ade2-101 his3-<math>\Delta</math>200 leu2-<math>\Delta</math>1 ura3-52 tub1-803-LEU2 tub3<math>\Delta</math>::HIS3</i>	This study
DBY6824	<i>MATa</i> <i>lys2-801 ade2-101 his3-<math>\Delta</math>200 leu2-<math>\Delta</math>1 ura3-52 tub1-804-LEU2 tub3<math>\Delta</math>::HIS3</i>	This study
DBY6826	<i>MATa</i> <i>lys2-801 ade2-101 his3-<math>\Delta</math>200 leu2-<math>\Delta</math>1 ura3-52 tub1-805-LEU2 tub3<math>\Delta</math>::HIS3</i>	This study
DBY6828	<i>MATa</i> <i>lys2-801 ade2-101 his3-<math>\Delta</math>200 leu2-<math>\Delta</math>1 ura3-52 tub1-806-LEU2 tub3<math>\Delta</math>::HIS3</i>	This study
DBY6830	<i>MATa</i> <i>lys2-801 ade2-101 his3-<math>\Delta</math>200 leu2-<math>\Delta</math>1 ura3-52 tub1-807-LEU2 tub3<math>\Delta</math>::HIS3</i>	This study
DBY6838	<i>MATa</i> <i>lys2-801 ade2-101 his3-<math>\Delta</math>200 leu2-<math>\Delta</math>1 ura3-52 tub1-811-LEU2 tub3<math>\Delta</math>::HIS3</i>	This study
DBY6840	<i>MATa</i> <i>lys2-801 ade2-101 his3-<math>\Delta</math>200 leu2-<math>\Delta</math>1 ura3-52 tub1-812-LEU2 tub3<math>\Delta</math>::HIS3</i>	This study
DBY6846	<i>MATa</i> <i>lys2-801 ade2-101 his3-<math>\Delta</math>200 leu2-<math>\Delta</math>1 ura3-52 tub1-815-LEU2 tub3<math>\Delta</math>::HIS3</i>	This study
DBY6854	<i>MATa</i> <i>lys2-801 ade2-101 his3-<math>\Delta</math>200 leu2-<math>\Delta</math>1 ura3-52 tub1-819-LEU2 tub3<math>\Delta</math>::HIS3</i>	This study
DBY6866	<i>MATa</i> <i>lys2-801 ade2-101 his3-<math>\Delta</math>200 leu2-<math>\Delta</math>1 ura3-52 tub1-825-LEU2 tub3<math>\Delta</math>::HIS3</i>	This study
DBY6868	<i>MATa</i> <i>lys2-801 ade2-101 his3-<math>\Delta</math>200 leu2-<math>\Delta</math>1 ura3-52 tub1-826-LEU2 tub3<math>\Delta</math>::HIS3</i>	This study
DBY6878	<i>MATa</i> <i>lys2-801 ade2-101 his3-<math>\Delta</math>200 leu2-<math>\Delta</math>1 ura3-52 tub1-831-LEU2 tub3<math>\Delta</math>::HIS3</i>	This study
DBY6880	<i>MATa</i> <i>lys2-801 ade2-101 his3-<math>\Delta</math>200 leu2-<math>\Delta</math>1 ura3-52 tub1-832-LEU2 tub3<math>\Delta</math>::HIS3</i>	This study
DBY6882	<i>MATa</i> <i>lys2-801 ade2-101 his3-<math>\Delta</math>200 leu2-<math>\Delta</math>1 ura3-52 tub1-833-LEU2 tub3<math>\Delta</math>::HIS3</i>	This study
DBY6886	<i>MATa</i> <i>lys2-801 ade2-101 his3-<math>\Delta</math>200 leu2-<math>\Delta</math>1 ura3-52 tub1-835-LEU2 tub3<math>\Delta</math>::HIS3</i>	This study
DBY6894	<i>MATa</i> <i>lys2-801 ade2-101 his3-<math>\Delta</math>200 leu2-<math>\Delta</math>1 ura3-52 tub1-839-LEU2 tub3<math>\Delta</math>::HIS3</i>	This study
DBY6898	<i>MATa</i> <i>lys2-801 ade2-101 his3-<math>\Delta</math>200 leu2-<math>\Delta</math>1 ura3-52 tub1-841-LEU2 tub3<math>\Delta</math>::HIS3</i>	This study
DBY6902	<i>MATa</i> <i>lys2-801 ade2-101 his3-<math>\Delta</math>200 leu2-<math>\Delta</math>1 ura3-52 tub1-843-LEU2 tub3<math>\Delta</math>::HIS3</i>	This study
DBY6916	<i>MATa</i> <i>lys2-801 ade2-101 his3-<math>\Delta</math>200 leu2-<math>\Delta</math>1 ura3-52 tub1-850-LEU2 tub3<math>\Delta</math>::HIS3</i>	This study
DBY6918	<i>MATa</i> <i>lys2-801 ade2-101 his3-<math>\Delta</math>200 leu2-<math>\Delta</math>1 ura3-52 tub1-851-LEU2 tub3<math>\Delta</math>::HIS3</i>	This study
DBY6920	<i>MATa</i> <i>lys2-801 ade2-101 his3-<math>\Delta</math>200 leu2-<math>\Delta</math>1 ura3-52 tub1-852-LEU2 tub3<math>\Delta</math>::HIS3</i>	This study
DBY7830	<i>MAT<math>\alpha</math></i> <i>lys2-801 ade2-101 his3-<math>\Delta</math>200 leu2-<math>\Delta</math>1 ura3-52 TUB1-LYS2 tub2-201</i> plasmid: pRB326	Schwartz <i>et al.</i> , 1997
DBY7051	<i>MATa</i> <i>ACT1::HIS his3-<math>\Delta</math>200 leu2-3,112 ura3-52 ade4 tub2-201</i>	This laboratory
DBY8154	<i>MATa</i> <i>lys2-801 ade2-101 his3-<math>\Delta</math>200 leu2-<math>\Delta</math>1 ura3-52 TUB1-LEU2 tub2-201</i>	This study

**Table 3.** Summary of mutations

<i>tub1</i> allele	Amino acid substitutions	DNA sequence changes <sup>a</sup>	Diagnostic restriction sites	Phenotype <sup>b</sup>
801	R2A, E3A	<u>GCTGCA</u> <u>AGAGAA</u>	Gain <i>Pst</i> I	Cs, Ts, BenSS
802	E27A, H28A	<u>GCAGCC</u> <u>GAGCAC</u>	Gain <i>Bbv</i> I	RL
803	K31A, D33A	<u>GCGCCGGCT</u> <u>AAGCCGGAT</u>	Gain <i>Hin</i> P1I, Lose <i>Bsa</i> BI	BenSS
804	H35A, E37A, D38A	<u>GCTCTAGCAGCT</u> <u>CATCTAGAAGAT</u>	Gain <i>Pvu</i> II, Lose <i>Bsa</i> BI	BenSS
805	K42A, K44A	<u>GCGCCGGCG</u> <u>AAGCCGAAG</u>	Gain <i>Hin</i> P1I	BenSS
806	E47A, E48A	<u>GCAGCT</u> <u>GAAGAG</u>	Gain <i>Pvu</i> II	BenR
807	H55A, E56A	<u>GCTGCA</u> <u>CATGAA</u>	Gain <i>Bbv</i> I	BenSS
808	K61A, R65A	<u>GCGTTCGTTCCAGCT</u> <u>AAGTTCGTTCCAAGG</u>	Gain <i>Pvu</i> II	RL
809	D70A, E72A	<u>GCTTTAGCG</u> <u>GATTTAGAG</u>	Gain <i>Hin</i> P1I	Slow growth, BenSS
810	D77A, E78A, R80A	<u>GCAGCAGTCGCT</u> <u>GACGAAGTCCGT</u>	Gain <i>Bbv</i> I	BenSS
811	K85A, D86A	<u>GCTGCC</u> <u>AAGGAC</u>	Gain <i>Bbv</i> I	WT
812	H89A, E91A	<u>GCTCCAGCA</u> <u>CATCCAGAA</u>	Gain <i>Bpm</i> I	BenSS
813	K97A, E98A, D99A	<u>GCGGCGGCC</u> <u>AAGGAGGAC</u>	Gain <i>Not</i> I	Slow growth, BenSS
814	R106A, H108A	<u>GCTGGCGCT</u> <u>AGAGGCCAT</u>	Gain <i>Pvu</i> II	Slow growth, BenSS
815	R113A, E114A	<u>GCAGCA</u> <u>AGAGAA</u>	Gain <i>Bbv</i> I	WT
816	D118A, D121A, R122A	<u>GCTGTTCTGGCTGCG</u> <u>GATGTTCTGGATAGG</u>	Gain <i>Bbv</i> I	Cs, BenSS
817	R124A, K125A	<u>GCAGCA</u> <u>AGAAAA</u>	Gain <i>Bbv</i> I	BenSS
818	D128A, D131A	<u>GCCCAATGTGCA</u> <u>GACCAATGTGGAT</u>	Gain <i>Bsg</i> I	Cs, BenSS
819	T146A	<u>GCA</u> <u>ACT</u>	Gain <i>Bsg</i> I, <i>Bsp</i> MI	BenSS
820	E156A, E157A	<u>GCAGCA</u> <u>GAAGAA</u>	Gain <i>Bbv</i> I	DL
821	E161A, K164A, K165A	<u>GCATACGGTGCGGCA</u> <u>GAATACGGTAAGAAA</u>	Gain <i>Fnu</i> 4HI	BenSS
822	K167A, E169A	<u>GCGCTGGCA</u> <u>AAGCTGGAA</u>	Gain <i>Hin</i> P1I	Slow growth, BenSS
823	E197A, H198A, D200A	<u>GCAGCTGCAGCT</u> <u>GAACATGCAGAT</u>	Gain <i>Pst</i> I, <i>Pvu</i> II	RL
824	D206A, E208A	<u>GCGAATGCG</u> <u>GATAATGAG</u>	Gain <i>Nru</i> I, <i>Bsm</i> I	Cs, BenSS
825	D212A, K215A, R216A	<u>GCCATGTGCGCAGCA</u> <u>GACATGTGCAAAAAGA</u>	Gain <i>Bbv</i> I	BenR
826	D219A, R222A	<u>GCTATCCCAGCA</u> <u>GATATCCAAGA</u>	Lose <i>Eco</i> RV	BenR
827	R244A, D246A	<u>GCAATCGCG</u> <u>AGATTCGAG</u>	Gain <i>Bst</i> UI	Slow growth, BenSS
828	D252A, E255A	<u>GCTTTGAACGCG</u> <u>GATTTGAACGAA</u>	Gain <i>Mlu</i> I	DL
829	R265A, H267A	<u>GCAATTGCT</u> <u>AGAATTCAT</u>	Gain <i>Mun</i> I, Lose <i>Eco</i> RI	Slow growth, BenSS
830	K279A, K281A	<u>GCATCAGCT</u> <u>AAATCAAAG</u>	Gain <i>Pvu</i> II	BenSS

(Continues)

Table 3. (Continued)

<i>tub1</i> allele	Amino acid substitutions	DNA sequence changes <sup>a</sup>	Diagnostic restriction sites	Phenotype <sup>b</sup>
831	H284A,E285A	<u>GCTGCG</u> <u>CATGAG</u>	Gain <i>Fnu4HI</i> , Lose <i>Hinfl</i> , <i>PleI</i>	Cs, BenSS
832	K305A, D307A	<u>GCGTGTGCA</u> <u>AAGTGTGAT</u>	Gain <i>ApaI</i>	BenR
833	R309A, D310A, K312A	<u>GCAGCTGGTGCA</u> <u>AGAGATGGTAAA</u>	Gain <i>PvuII</i> , <i>Fnu4HI</i>	BenSS
834	R321A, D323A	<u>GCGGGTGCT</u> <u>AGGGGTGAT</u>	Gain <i>BstUI</i>	Slow growth, BenSS
835	R327A, D328A, R331A	<u>GCTGTTCAAGCA</u> <u>GATGTTCAAAGA</u>	Gain <i>PvuII</i>	WT
836	E334A, K337A	<u>GCGCAGGTGGCA</u> <u>GAGCAGGTGAAA</u>	Gain <i>BstUI</i> , <i>HinPII</i>	Cs, Ts, BenSS
837	K339A, K340A	<u>GCGGCG</u> <u>AAGAAG</u>	Gain <i>Fnu4HI</i> , <i>BstUI</i> , Lose <i>BbsI</i>	BenSS
838	D373A, R374A	<u>GCTGCA</u> <u>GATAGG</u>	Gain <i>PstI</i> , <i>SfcI</i>	BenSS
839	E387A, K390A, R391A	<u>GCAGCTTGGGCGGCA</u> <u>GAGGCTTGGAAAGAGA</u>	Gain <i>PstI</i>	BenR
840	D393A, R394A, K395A, D397A	<u>GCTGCAGCATTCGCT</u> <u>GATAGAAAAATTCGAT</u>	Gain <i>PstI</i> , <i>BsmI</i> , <i>SfcI</i> , Lose <i>ClnI</i>	RL
841	D393A, R394A	<u>GCTGCA</u> <u>GATAGA</u>	Gain <i>PstI</i>	BenR
842	K395A, D397A	<u>GCATTCGCT</u> <u>AAATTCGAT</u>	Gain <i>BsmI</i>	Cs, Ts, BenSS
843	K395A	<u>GCA</u> <u>AAA</u>	Gain <i>BsmI</i>	WT
844	D397A	<u>GCA</u> <u>GAT</u>	Gain <i>AseI</i>	BenSS
845	K402A, R403A	<u>GCAGCT</u> <u>AAACGT</u>	Gain <i>PvuII</i>	Slow growth, BenSS
846	E412A, E415A	<u>GCAGGTATGGCA</u> <u>GAAGGTATGGAA</u>	Gain <i>BsgI</i> , <i>BspMI</i>	Cs, Ts, BenSS
847	E416A, E418A	<u>GCAGGTGCA</u> <u>GAAGGTGAA</u>	Gain <i>BsmI</i> , <i>BspMI</i> , Lose <i>EcoRI</i>	Slow growth, BenSS
848	E421A, R423A, E424A, D425A	<u>GCAGCTGCAGCAGCT</u> <u>GAAGCTAGAGAAGAT</u>	Gain <i>PstI</i> , <i>PvuII</i>	Slow growth, BenSS
849	E430A, R431A, D432A	<u>GCTGCAGCT</u> <u>GAAAGAGAT</u>	Gain <i>PstI</i>	Slow growth, BenSS
850	E435A, D439A	<u>GCGGTGGGTGCCGCC</u> <u>GAAGTGGGTGCCGAC</u>	Gain <i>BstUI</i>	BenSS
851	E443A, E444A, E445A, E446A	<u>GCTGCAGCGGCA</u> <u>GAGGAAGAGGAA</u>	Gain <i>PstI</i>	BenSS
852	F447A	<u>GCT</u> <u>TTT</u>	Gain <i>HindIII</i>	BenSS
853	E184A	<u>GCG</u> <u>GAG</u>	Gain <i>HinPII</i>	Slow growth, BenSS

<sup>a</sup> The mutant sequence is above the corresponding wild-type sequence. Altered nucleotides are in bold; altered codons are underlined.

<sup>b</sup> BenR, benomyl resistant; BenSS, benomyl supersensitive; Cs, cold-sensitive; DL, dominant lethal; RL, recessive lethal; Slow growth, impaired growth at all temperatures; Ts, heat-sensitive; WT, wild-type.

Two haploids with each *tub1* mutant, one of each mating type, were mated to a *tub3Δ* strain; MAT $\alpha$  *tub1* strains were mated to DBY6598, and MAT $\alpha$  *tub1* strains were mated to DBY6599. The *tub1 tub3Δ* double mutants (DBY6816 through DBY6920) are haploid progeny of these crosses.

### DNA Manipulation

All restriction enzymes, T4 ligase, T7 polymerase, and Klenow were from New England Biolabs (Beverly, MA). Calf intestinal phosphatase was from Boehringer Mannheim (Indianapolis, IN). *Taq* poly-

merase was from Perkin Elmer-Cetus (Foster City, CA) or Life Technologies (Santa Clara, CA). Buffers were either used as supplied or remade according to the manufacturer's specifications. Nucleotides were from Pharmacia (Alameda, CA). Oligonucleotide primers were supplied by Genset (La Jolla, CA).

### Site-directed Mutagenesis

Methods were modified from those of Kunkel *et al.* (1987) and Sambrook *et al.* (1989) and are described in detail elsewhere (Miller *et al.*, 1996). Briefly, an oligonucleotide bearing the desired mutation (see Table 3) was annealed to a single-stranded DNA template, pRB2065, containing a high frequency of uracil misincorporations. Oligonucleotides were designed with at least 12 bp of homology on either side of the altered nucleotides. Synthesis of the second strand, primed by the mutant oligonucleotide, was done *in vitro*, and the product was transformed into an *Escherichia coli* strain able to recognize and repair the uracil misincorporations. The repair process resulted in coding information from the template (wild-type) strand being replaced with the coding information from the mutant strand. Resultant plasmids were screened for the introduction or loss of a restriction site to identify those with the desired mutation.

### Construction of *tub1* Strains

*tub1* mutant plasmids, digested with *Sph*I and *Sac*I to release the fragment containing the *tub1* and downstream *LEU2* integration, were transformed into DBY6596, and Leu<sup>+</sup> transformants were selected. DBY6596 is a heterozygous diploid with a *HIS3*-marked *tub1* deletion (*tub1*Δ::*HIS3*) on one chromosome XIII; on the homologue, the wild-type *TUB1* locus marked by *LYS2* integrated downstream. In this diploid, a *TUB1* centromeric plasmid, pRB326, is maintained to prevent the aneuploidy that results from propagating strains heterozygous for a *tub1* deletion (Schatz *et al.*, 1986b). The transforming *tub1*-*LEU2* fragment could integrate by homologous recombination at any of the three *TUB1* loci (two chromosomal and one plasmid) in the recipient strain. The desired integration event was recovered by screening Leu<sup>+</sup> transformants that had become His<sup>-</sup> as a result of the replacement of the *tub1*Δ::*HIS3* allele. This screening also eliminated any unwanted products of illegitimate recombination (i.e., integrations at loci other than *TUB1*).

The resultant diploids are heterozygous for the *tub1* mutation. In addition, both the wild-type and mutant *TUB1* loci are marked by *LYS2* and *LEU2*, respectively. These auxotrophic markers were inserted ~1 kb downstream of *TUB1* and therefore remain tightly linked to *TUB1* during meiotic segregation, allowing for convenient identification of *tub1*-containing haploid segregants. These markers can also readily reveal any chromosome XIII aneuploidy, because Lys<sup>+</sup> and Leu<sup>+</sup> do not segregate 2:2 under those conditions. It should be noted that insertion of these auxotrophic marker genes disrupts the open reading frame downstream of *TUB1*. This gene, *ALO1*, encodes D-arabino-1,4-lactone oxidase, which catalyzes the biosynthesis of D-erythroascorbic acid in yeast (Huh *et al.*, 1998). This disruption had no microtubule phenotype on its own, and all *tub1* alleles were compared with the appropriate control, a strain with a wild-type *TUB1* gene marked by the downstream auxotrophic marker insertion in *ALO1*.

To assess viability in the absence of the plasmid-borne *TUB1* gene, the heterozygous diploids and the dissection plates containing haploid segregants were replica plated to medium containing 5-fluoroorotic acid (5-FOA), which selects against the *URA3*-marked pRB326 plasmid. Each dissection plate was also replica plated to mating-type tester lawns and onto media to test for the various auxotrophic markers. The auxotrophic markers indicate which haploid segregants carry pRB326 and whether they carry the wild-type (Lys<sup>+</sup>) or mutant (Leu<sup>+</sup>) *TUB1* gene.

Each mutant was constructed twice independently. Both independent isolates of each haploid mutant, and occasionally the heterozygous diploid parent, were verified by PCR amplification of the

*TUB1* gene followed by a restriction digest to verify the presence of the restriction site introduced by that particular mutation (Table 3). This test also confirmed the absence of the wild-type *TUB1* gene in the haploids.

### Yeast Transformation

Yeast were transformed using electroporation (Becker and Guarente, 1991), using ~1–2 μg of DNA per transformation. For constructing parental strains and for making the first isolate of each Ala-scan mutant, the DNA usually came from a gel-purified fragment. The DNA was purified using the Qiaex (Qiagen, Chatsworth, CA) DNA purification system. For the second isolate of each mutation (and sometimes for the first isolate as well), the DNA was digested from a crude minipreparation of DNA, ethanol precipitated, and transformed directly without purification of the transforming fragment.

### Colony PCR to Verify Mutation

Genomic DNA was amplified directly from yeast colonies by resuspending a colony directly into 5 μl of water in a PCR tube and immediately placing it on ice. A mixture of all the other components was prepared on ice. The mixture was composed such that adding 25 μl to the 5 μl of cells would produce a final concentration of 0.25 μM of each primer, 2.5 U of *Taq* polymerase, 1× *Taq* buffer (10 mM Tris-HCl, pH 8.5, 50 mM KCl, and 1.5 mM MgCl<sub>2</sub>), and 0.1 μg/μl BSA. Immediately after dividing the mixture into each reaction tube while on ice, the tubes were vortexed very briefly, mineral oil was added, and tubes were placed into a preheated (>90°C) DNA Thermal Cycler (Perkin Elmer-Cetus). The cycling conditions varied but worked best with 94°C, 4 min, 30 cycles (92°C, 1 min; 55°C, 1 min; and 72°C, 2 min); 72°C, 20 min; and a 4°C soak.

Half of the reaction product (15 μl) was digested with the appropriate restriction enzyme (see Table 3) in a final reaction volume of 20 μl, and the entire reaction was run on an agarose gel to verify the presence or absence of the restriction site resulting from the particular *tub1* mutation.

### DNA Sequencing of *tub2-201*

*tub2-201* DNA was PCR amplified from strains DBY7051 (twice) and DBY8154 (once) using *Taq* polymerase (Life Technologies, Rockville, MD) and primers KStub2-01 (5'-GCGCCATGGAGATGAGAGAAAT-CATTCAT-3') and KStub2-02 (5'-GCGCCATGGTTATTCAAAT-TCTCAGTGATTGG-3'), which anneal to the first and last 18 nucleotides of the *TUB2* open reading frame. Products from independent amplifications were cloned into the *Nco*I site of pACTII (Bai and Elledge, 1996), resulting in three *tub2-201*-containing plasmids. The 5'- and 3'-most ends of the *tub2-201* open reading frame were PCR amplified using primers KStub2-03 (5'-GCGGGATCCGTAGTGGTGAG-GCAATTGG-3'), KStub2-04 (5'-CCGCTAGACGAGATCAAAAAGC-GTACC-3'), KStub2-05 (5'-GCGGGATCCCCCAACAATGTGCA-AAC-3'), and KStub2-06 (5'-GCGTCTAGATTTATTTTGCTCCA-AGTGC-3'). Purified *tub2-201* DNA (plasmid or PCR product) was sequenced with ThermoSequenase dye terminator cycle sequencing mix (Amersham, Arlington Heights, IL) and an ABI PRISM 373XL DNA sequencer (Applied Biosystems, Foster City, CA) according to the manufacturer's instructions.

### Immunofluorescence Microscopy

Visualization of microtubules with indirect immunofluorescence and 4',6'-diamidino-2-phenylindole (DAPI) staining to visualize nuclei were performed as described previously (Schwartz *et al.*, 1997).

### Growth Rate Measurement

Growth rates were determined by diluting 1 ml of a dense YPD culture into 24 ml of YPD, incubating with agitation for 2–3 h to allow cells to begin growing exponentially, and then splitting the

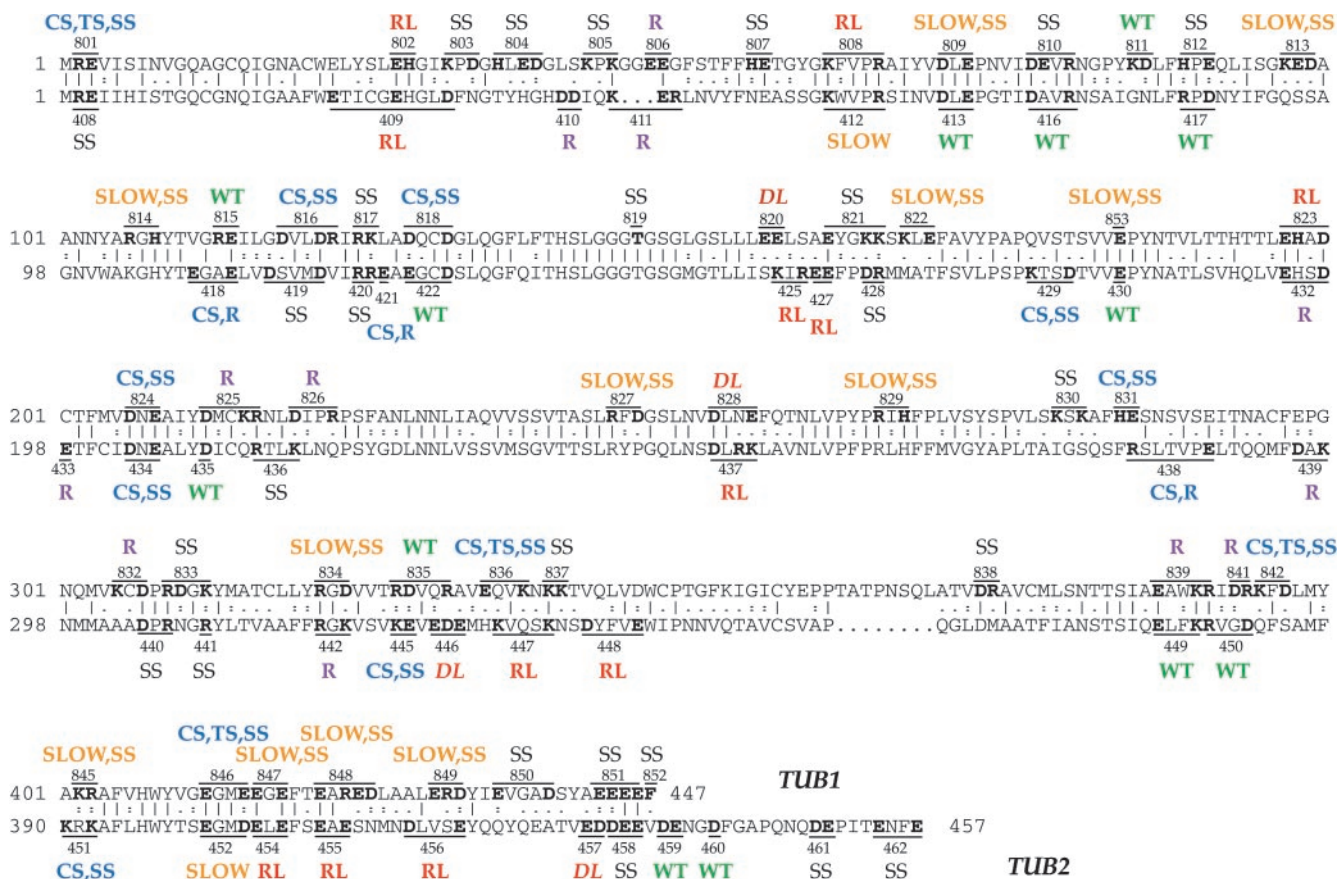


**Figure 1.** Phenotypes of *TUB1* and *TUB2* Ala-scan mutants. The positions of the mutations and their resulting phenotypes are shown for both *TUB1* (top) and *TUB2* (bottom). The allele number of each mutation is shown, and the altered residues are in bold. SS, benomyl-supersensitive; R, benomyl-resistant; WT, wild-type; CS, cold-sensitive; TS, heat-sensitive; SLOW, slow growth at all temperatures. The *TUB2* Ala-scan data is reproduced from Reijo *et al.* (1994), and phenotype definitions are adapted to be identical to those used in describing the *TUB1* mutants.

culture three ways: 8 ml of culture into 17 ml of YPD to be incubated at 11, 25, and 37°C. Readings were taken periodically with a Klett (New York, NY) colorimeter, and growth was plotted using Cricket Graph 1.3.2 (Cricket Software, Malvern, PA). The equation of the growth curve was used to calculate a doubling time for each strain.

### Bud Index Determination

Cells were diluted from a saturated culture and incubated 3–4 h to allow cells to begin exponential growth. The cultures were then split and placed at 25 and 11°C. After two wild-type doubling times, the cells were counted using a hemacytometer. The bud index was simultaneously obtained by counting at least 200 cells and categorizing them as unbudded, small-budded, medium-budded (a bud diameter greater than one-fourth of the diameter of the mother cell body), or large-budded (a bud diameter greater than one-half of the diameter of the mother cell body).

### Spot Replica Plating

Cells were grown in 2 ml of YPD for 36–48 h. to allow all cultures to arrive at approximately the same density. All cultures were diluted into wells of a microtiter dish, producing  $10^{-1}$  and  $10^{-3}$  dilutions of each culture. These dilutions were plated using a 12-

channel multipipettor, dispensing 3  $\mu$ l per spot. Plates were observed and photographed daily to record data.

### Molecular Modeling

The structure of the  $\alpha$ - $\beta$ -tubulin heterodimer from bovine brain was obtained by electron crystallography of zinc-induced tubulin sheets stabilized with taxol (Nogales *et al.*, 1998b). Tub1p and Tub2p sequences were modeled with the LOOK software package (Molecular Applications Group, Palo Alto, CA) using the coordinates from the solved bovine tubulin structure as a template. Five hundred rounds of energy minimization refinements were used. GTP and GDP, but not taxol, were included in the model. The C termini of Tub1p (residues 442–447) and Tub2p (residues 428–457) were not included in the model, because they are not resolved in the current bovine tubulin structure (Nogales *et al.*, 1998b). The resulting yeast tubulin model was quite similar to the bovine tubulin crystal structure: the root mean square deviation for 2601 polypeptide backbone atoms was 1.21 Å as calculated with Swiss-PdbViewer (Guex and Peitsch, 1997). The coordinates of this yeast tubulin model, along with interactive views of the model, are available at the Botstein laboratory web site: <http://genome-www.stanford.edu/group/botlab/tubulin>.

## RESULTS AND DISCUSSION

### *Design and Construction of Charged-to-Ala Scan Mutations*

Mutations were designed by examining the protein sequence of Tub1p, inspecting each window of five amino acids for two or more "charged" residues (we included H as well as K, R, D, and E). Mutations were designed to replace all of these "clustered charged" residues with alanine while minimizing the total number of mutations. As a result, each mutation changed two to four residues from charged to alanine. Only 10 charged residues were not included within any of the alanine-scanning mutations, and only one of these (H407) was within five amino acids of another charged residue. Residue E184, although not within a charged cluster, was mutated because it is in the middle of an extremely well-conserved sequence present in all tubulins ( $\alpha$ ,  $\beta$ , and  $\gamma$ ): VVEPYN. *tub1-842* was subdivided into two additional mutations, changing K395 and D397 separately (*tub1-843* and *tub1-844*). Based on sequence conservation, these two residues may be important for  $\alpha$ -tubulin-specific functions (Cleveland *et al.*, 1990; Burns, 1991), and in addition, K395 has been shown to be an important residue for microtubule assembly (Sherman *et al.*, 1983; Szasz *et al.*, 1986).

Other noncharged residues were also mutated to alanine. T146 (mutated to A in *tub1-819*) is part of the tubulin signature sequence (GGGTGSG) (Bairoch, 1991), an invariant sequence found in every tubulin gene discovered to date. This sequence is now known to form part of the GTP-binding site by interacting with the nucleotide's phosphates (Nogales *et al.*, 1998a,b). *tub1-852* changes the last residue of Tub1p, a phenylalanine, to an alanine. This C-terminal residue is the subject of post-translational modification in vertebrate  $\alpha$ -tubulins (Arce *et al.*, 1978; Argarana *et al.*, 1978; Barra *et al.*, 1988).

During the construction of these mutations, two sequencing errors were discovered in the published *TUB1* sequence (Schatz *et al.*, 1986a). The first changes Leu-94(CTC) to Ile-94(ATC), and the second changes Thr-326 Gly-327(ACG GGA) to Thr-326 Arg-327(ACA AGA). Both of these amino acid changes increase the identity of Tub1p with Tub3p. Both of these nucleotide changes were also found by the systematic sequencing effort, as reported in the chromosome XIII sequence (Bowman *et al.*, 1997).

A total of 53 mutations were constructed by site-directed mutagenesis and then integrated into the *TUB1* locus by homologous recombination, resulting in *tub1/TUB1* heterozygotes (see MATERIALS AND METHODS). Each mutant was constructed twice independently and was subjected to the same initial phenotypic characterization to be sure the phenotypes of the two isolates agreed. This guarded against misinterpretation attributable to second-site mutations introduced sometime during the mutagenesis procedure, because the likelihood of this occurring in two independent isolates is minimal. A *TUB1* centromeric plasmid (pRB326) was maintained in these strains during their construction to prevent aneuploidy, which results from propagating strains heterozygous for *tub1* null alleles (Schatz *et al.*, 1986b). Once the mutants were constructed, the phenotypes of these diploids and their haploid progeny were assessed in the absence of the plasmid-borne *TUB1* by plating on 5-FOA, which selects against the *URA3*-marked pRB326 plasmid.

### *tub1 Mutant Phenotypes*

The phenotype of the *tub1* haploids was characterized by testing for growth at different temperatures ranging from 11 to 37°C, and on media containing benomyl concentrations ranging from 2 to 50  $\mu\text{g}/\text{ml}$ . Benomyl is a member of the benzimidazole family of microtubule-destabilizing drugs and is known to affect the growth of many tubulin mutants in yeast (Thomas *et al.*, 1985; Schatz *et al.*, 1988), although its exact mechanism of action is unknown. Growth rates in liquid medium were determined for each viable mutant at 11, 25, and 37°C. Each mutant was then classified as cold-sensitive (Cs) if growth was impaired at 11°C, temperature-sensitive (Ts) if growth was impaired at 37°C, and slow-growing if growth was impaired at 25°C as well as at extreme temperatures. In addition, each mutant was classified as benomyl-supersensitive if growth was impaired relative to wild type on media containing benomyl and benomyl-resistant if growth was better than wild type on media containing benomyl.

The phenotypes resulting from each *tub1* mutation are shown in Figure 1 and Table 3. Two were dominant lethal mutations, because the diploid transformants, heterozygous for the mutation, were unable to grow without additional copies of *TUB1* (pRB326) and therefore died on 5-FOA. Four were recessive lethal mutations; the haploid *tub1* segregants failed to grow without the *TUB1* plasmid on 5-FOA. Twenty-one alleles produced a conditional growth phenotype (Cs, both Cs and Ts, or impaired over the entire temperature range). Growth of each of these mutants at various temperatures is shown in Figure 2. Almost all of the mutations show an altered sensitivity to benomyl. Wild-type haploids (e.g., DBY6654 and DBY6655) grew well on concentrations of benomyl up to 20  $\mu\text{g}/\text{ml}$  and grew weakly on a concentration of 30  $\mu\text{g}/\text{ml}$ . Six strains, those containing the alleles *tub1-806*, *-825*, *-826*, *-832*, *-839*, and *-841*, grew well on 30  $\mu\text{g}/\text{ml}$  benomyl and were therefore benomyl resistant. Despite previous extensive mutagenesis of *TUB1* (Schatz *et al.*, 1988), these are the first benomyl-resistant *tub1* alleles isolated. These strains were not completely insensitive to benomyl, however, because they failed to grow on 75  $\mu\text{g}/\text{ml}$  benomyl. Most of the other *tub1* mutants were more benomyl sensitive than wild type, failing to grow on 20  $\mu\text{g}/\text{ml}$  benomyl. We placed the *tub1* mutants into five categories based on their benomyl sensitivities relative to wild type and the benomyl-supersensitive mutant *tub3 $\Delta$*  (which failed to grow on 10  $\mu\text{g}/\text{ml}$  benomyl). The categories were, in descending degree of sensitivity: 1) more sensitive than *tub3 $\Delta$* , 2) approximately equal in sensitivity to *tub3 $\Delta$* , 3) less sensitive than *tub3 $\Delta$*  but more sensitive than wild type, 4) approximately equal in sensitivity to wild type, and 5) less sensitive than wild type (i.e., benomyl-resistant) (Table 4). Because nearly all of these systematic *tub1* mutations alter benomyl sensitivity, it appears that microtubules are exquisitely sensitive to changes in Tub1p sequence.

### *Synthetic Lethality with Deletions of TUB3*

To determine the phenotype of each *tub1* allele in the absence of any wild-type  $\alpha$ -tubulin, each was combined with a deletion of the minor  $\alpha$ -tubulin gene *TUB3*. The resulting phenotypes are shown in Table 4. None of the lethal *tub1* mutants was rescued by removing *TUB3*. Remarkably, more

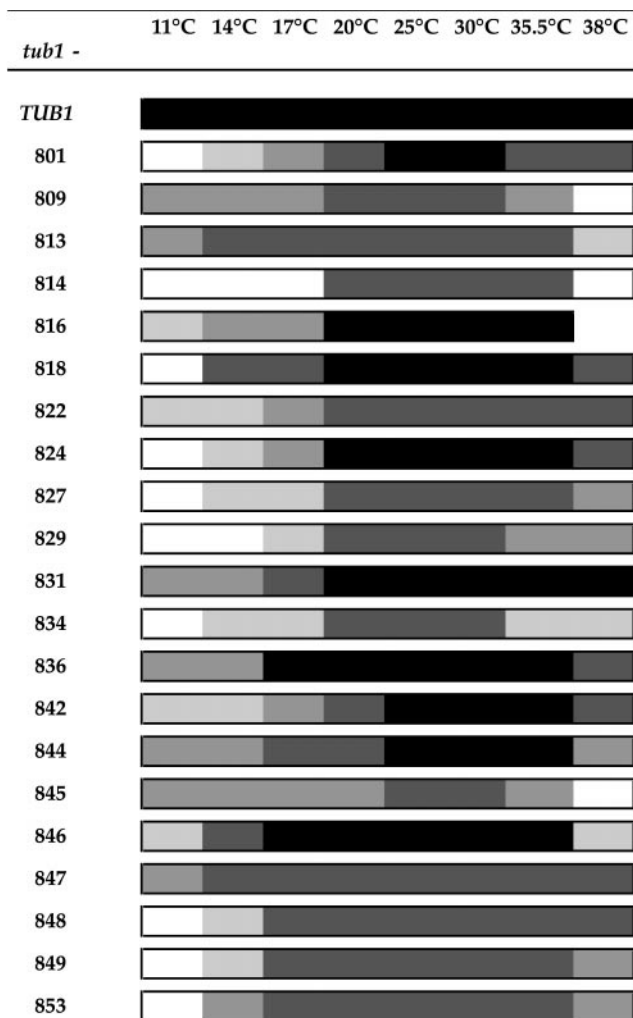


**Figure 2.** Growth of *tub1* mutants at various temperatures. The growth of each mutant was compared with the growth of the wild-type control across a range of temperatures. Growth ranges from wild-type growth (heavily shaded) to no growth (unshaded).

than half of the viable *tub1* mutants (26 of 47) were synthetically lethal in combination with *tub3Δ*. Furthermore, many of the remaining viable *tub1 tub3Δ* double mutants were severely growth impaired. *TUB3* obviously plays a vital role in the microtubule function of most of the *tub1* mutants.

Categorizing the *tub1* mutants according to their degree of benomyl supersensitivity was a very good predictor of the viability of the *tub1 tub3Δ* double mutant. Alongside each mutant allele in Table 4 are any temperature and/or cold sensitivities produced by that allele, as well as its *tub3Δ* double mutant phenotype. Almost without exception, the most benomyl-supersensitive and growth-impaired *tub1* alleles are also the alleles that are synthetically lethal with *tub3Δ*. The most parsimonious explanation for this observation is that the phenotypic effect of removing *TUB3* from *tub1* strains is merely additive, so that the most severe *tub1* alleles will not be able to tolerate it, whereas the less severe alleles will. The exceptions to this rule may indicate *TUB1*-

**Table 4.** *tub1* and *tub1 tub3* mutant phenotypes

Category of benomyl sensitivity <sup>a</sup>	<i>tub1</i> allele	<i>tub1</i> phenotype <sup>b</sup>	<i>tub1 tub3Δ</i> phenotype <sup>b</sup>	
1	801	BenSS, Cs, Ts	SL	
	809	BenSS, slow	SL	
	813	BenSS, slow	SL	
	814	BenSS, slow	SL	
	817	BenSS	SL	
	822	BenSS, slow	SL	
	824	BenSS, Cs	SL	
	827	BenSS, slow	SL	
	829	BenSS, slow	SL	
	833	BenSS	BenSS, slow	
	834	BenSS, slow	SL	
	836	BenSS, Cs, Ts	SL	
	2	810	BenSS	SL
		816	BenSS, Cs	SL
		818	BenSS, Cs	SL
		819	BenSS	BenSS, slow
		830	BenSS	SL
		837	BenSS	SL
		845	BenSS, slow	SL
846		BenSS, Cs, Ts	SL	
849		BenSS, slow	SL	
853		BenSS, slow	SL	
3	803	BenSS	BenSS, slow	
	804	BenSS	BenSS, Cs	
	805	BenSS	BenSS, slow	
	807	BenSS	BenSS, slow	
	812	BenSS	BenSS, Ts	
	821	BenSS	SL	
	831	BenSS, Cs	BenSS, slow	
	838	BenSS	SL	
	842	BenSS, Cs, Ts	SL	
	844	BenSS, Cs, Ts	SL	
	847	BenSS, slow	SL	
	848	BenSS, slow	SL	
	850	BenSS	BenSS, slow	
	851	BenSS	BenSS, slow	
	852	BenSS	BenSS	
4	<i>TUB1</i>	WT	BenSS	
	811	WT	BenSS	
	815	WT	BenSS	
	835	WT	BenSS	
	843	WT	BenSS, Cs	
5	806	BenR	BenSS	
	825	BenR	BenSS	
	826	BenR	BenSS	
	832	BenR	BenSS	
	839	BenR	BenSS	
	841	BenR	BenSS, slow	

<sup>a</sup> 1, more sensitive than *tub3Δ*; 2, sensitivity equal to *tub3Δ*; 3, less sensitive than *tub3Δ* but more sensitive than wild type; 4, sensitivity equal to wild type; 5, less sensitive than wild type (benomyl-resistant).

<sup>b</sup> BenR, benomyl resistant; BenSS, benomyl supersensitive; Cs, cold-sensitive; SL, synthetic lethal; slow, slow growth at all temperatures; Ts, heat-sensitive; WT, wild-type.

or *TUB3*-specific functional regions or may indicate regions where a particular residue is required, but only in a subset of  $\alpha$ -tubulin subunits. For example, the *tub1-844* mutant, although just slightly more benomyl-supersensitive than the

**Table 5.** Microtubule phenotypes of *tub1* mutants and *tub1 tub3Δ* double mutants

<i>tub1</i> mutant	Microtubule class	Growth phenotype	<i>tub1 tub3Δ</i> mutant	Microtubule class	Growth phenotype
800 (wild-type)	3	WT	800 <i>tub3Δ</i>	3	BenSS
801	3	BenSS, Cs, Ts	803 <i>tub3Δ</i>	1	BenSS, slow
806	3	BenR	805 <i>tub3Δ</i>	3	BenSS, slow
809	1	BenSS, slow	806 <i>tub3Δ</i>	3	BenSS
813	3	BenSS, slow	807 <i>tub3Δ</i>	1	BenSS, slow
814	3	BenSS, slow	812 <i>tub3Δ</i>	3	BenSS, Ts
822	3	BenSS, slow	819 <i>tub3Δ</i>	3	BenSS, slow
827	1	BenSS, slow	825 <i>tub3Δ</i>	3	BenSS
829	3	BenSS, slow	831 <i>tub3Δ</i>	3	BenSS, slow
831	2	BenSS, Cs	833 <i>tub3Δ</i>	3	BenSS, slow
834	1	BenSS, slow	850 <i>tub3Δ</i>	3	BenSS, slow
845	3	BenSS, slow	851 <i>tub3Δ</i>	1	BenSS, slow
846	3	BenSS, Cs, Ts	852 <i>tub3Δ</i>	3	BenSS
847	3	BenSS, slow			
848	3	BenSS, slow			
849	3	BenSS, slow			
853	3	BenSS, slow			

Microtubules from mutant cells grown for two generations at 11°C were visualized using indirect immunofluorescence. Intensity was scored in comparison with wild type (*TUB1-800*), which was included in every experiment. Mutants are divided into three categories according to their microtubule phenotypes: 1) very diminished or no microtubules, 2) excess microtubules, and 3) normal microtubules, sometimes fainter than usual. Growth phenotypes are shown for comparison, and abbreviations are as listed in Table 4.

wild-type, does not survive in the absence of *TUB3*. The residue altered by this allele may be crucial for microtubule function, but the few monomers encoded by *TUB3* are sufficient to allow microtubule function.

### Microtubule and Nuclear Phenotypes of Cold-sensitive *tub1* Mutants

The cold-sensitive *tub1* mutants were further examined by visualizing microtubules themselves with indirect immunofluorescence. Previously, *tub1* mutants were found to fall in three classes. Class 1 mutants had very few or no detectable microtubules, class 2 mutants had extra and/or longer microtubules, and class 3 mutants had relatively normal numbers of microtubules, sometimes disorganized. (Schatz *et al.*, 1988). This system provided a convenient classification scheme for organizing the current set of *tub1* mutants as well.

The microtubules were observed after fixing cells grown at the nonpermissive temperature. In general, the observed phenotypes agreed very well with the *tub1* mutant phenotype categories defined by Schatz *et al.* (1988). Several of the mutants displayed reduced or no staining at the restrictive temperature, indicating that they have impaired microtubule formation or stability. Many mutants, other than having an absence of long spindles, as would be predicted from the defect in nuclear division seen by DAPI staining (see below), displayed no other distinct microtubule phenotypes. One mutant, *tub1-831*, has brighter, more numerous, and longer than normal extranuclear microtubules throughout the cell cycle. This mutant phenotype is similar to the class 2 mutant microtubule phenotype described by Schatz *et al.* (1988). Table 5 shows the microtubule phenotypes of each of the *tub1* mutants.

Many of the cold-sensitive mutants were examined at the restrictive temperature (11°C) for nuclear phenotypes result-

ing from disrupted microtubules. Two primary microtubule defects, nuclear migration and nuclear division, were quantified using the DNA dye DAPI to visualize nuclei, and cell cycle progression was assessed by determining the distribution of bud sizes. Nuclear migration requires extranuclear microtubules (Huffaker *et al.*, 1988). In wild-type cells, nuclear migration happens early in the cell cycle, so large-budded cells are almost never observed without the nucleus at or extended through the bud neck. The other microtubule defect that was visualized with DAPI staining is in nuclear division, a process requiring intranuclear microtubules (Huffaker *et al.*, 1988). In tubulin mutants, when chromosomes do not separate because of a nonfunctional spindle, the nucleus does not divide. This is easily visualized as large-budded cells containing a single DAPI-staining region, rather than the two distinct DAPI-staining regions seen in wild-type large-budded cells.

The *tub1* mutants accumulate large-budded cells to varying degrees and show a variety of nuclear phenotypes, shown in Figure 3. Some mutants become dramatically worsened at 11°C; whereas some are equally affected at both temperatures. Some alleles produce defects predominantly in either nuclear division or nuclear migration, whereas some alleles affect both processes to the same extent. Analysis of these phenotypes leads to several general conclusions. First, the accumulation of large-budded cells, although not absolute, is significant in most of the *tub1* mutants, probably arising from a delay in mitosis. Second, the *tub3Δ* mutant has both a nuclear migration and a detectable nuclear division defect that is more severe at 11°C. This ability to distinguish a *tub3Δ* strain from the wild type demonstrates the sensitivity of this assay and reveals two new, albeit subtle, phenotypes for the *tub3Δ* mutant. Third, the *tub1 tub3Δ* double mutants have generally more severe

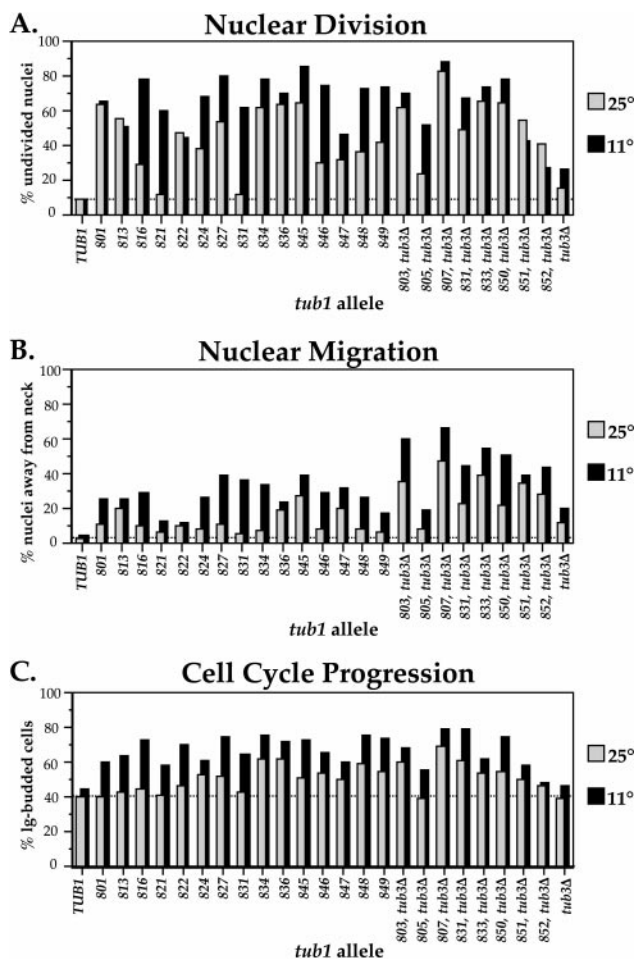


**Figure 3.** Nuclear phenotypes and cell cycle progression of *tub1* mutants. Large-budded cells were examined both by ascertaining their frequency in a growing population of cells and by staining their nuclei with DAPI. Cells were examined both at 25°C and after a shift to 11°C for two generations. In A, the percentage of large-budded cells with an undivided nucleus was determined; in B, the percentage of large-budded cells with a nucleus away from its normal position near the bud neck was determined; and in C, the percentage of large-budded cells (bud diameter greater than one-half of the mother cell's body) in the population was determined.

defects in nuclear migration than *tub1* mutants, in contrast with nuclear division, which is affected to the same degree. Last, the defects in nuclear division resulting from the *tub1* Ala-scan mutations are more dramatic than the defects in nuclear migration, in concordance with the results obtained from analysis of the *tub2* Ala-scan mutants.

### Comparison of *tub1* and *tub2* Mutant Phenotypes

Because microtubules are made of heterodimers of  $\alpha$ - and  $\beta$ -tubulin, it is worthwhile to compare the set of *TUB1* Ala-scan mutants and the set of *TUB2* Ala-scan mutants (Reijo *et al.*, 1994). It should be noted that direct comparisons between *tub1* and *tub2* mutant phenotypes are complicated by the existence of a second  $\alpha$ -tubulin gene (*TUB3*). None-

theless, there are several notable comparisons. First, both the *TUB1* and *TUB2* systematic mutageneses produced a few dominant lethal alleles. There were more recessive lethal alleles in *TUB2*, which is not surprising, given that *TUB2* is the sole  $\beta$ -tubulin gene, whereas *TUB3* provides a nontrivial fraction of the cell's  $\alpha$ -tubulin. Second, there are more *tub2* benomyl-resistant mutants. Mutations that simultaneously result in benomyl resistance and cold sensitivity were found only in *TUB2*. In *TUB1*, all of the benomyl-resistant mutants show wild-type growth at all temperatures. Finally, a much higher percentage of *tub1* mutants are benomyl supersensitive, leaving only three *tub1* mutants with a normal growth phenotype, many fewer than the number of normally growing *tub2* mutants.

The results of comparing analogous mutations in *TUB1* and *TUB2* are shown in Figure 1. Although the identical mutation was rarely made, it is nonetheless notable how dissimilar the results are across the entire length of the proteins. Six of the *tub1* mutations (*tub1*-801, -808, -809, -824, -847, and -853) are absolutely identical to their cognate *tub2* mutation, yet none of these shares the same phenotype with its *tub2* counterpart. There are three lethal *tub1* mutations that seem to be in essential regions shared between the two proteins (see *tub1*-802, -820, and -828), but in other cases (*tub1*-823 and *tub2*-454) the exact counterpart of a lethal mutation in one gene has a viable phenotype in the other gene. Furthermore, the dominant lethal *TUB1* mutations are in the N-terminal half of the protein, whereas the dominant lethal *TUB2* mutants are in the C-terminal half. This illustrates what appears to be an essentially complete functional divergence between the two components of the tubulin heterodimer, even though their three-dimensional structure is nearly identical and their primary sequence is very similar. This seems a natural consequence of the polarity of both the tubulin dimer and the microtubule and of the different involvement of  $\alpha$ - and  $\beta$ -tubulin in the interaction with other cellular components.

### Structure–Function Relationships

The amino acids altered by *tub1* and *tub2* systematic mutations were mapped onto a three-dimensional model (see MATERIALS AND METHODS) of the yeast tubulin dimer. Most of the mutated residues are distributed relatively evenly across the protein surface. Figure 4 illustrates this distribution for Tub1p; the distribution of mutations on Tub2p is similar. The longitudinal interfaces and the microtubule-interior face of each monomer have regions (10–15 Å in diameter) that are devoid of charged residues. A small fraction of the mutated residues are buried in the structure, including Tub1p residues R65, D70, T146, E169, D206, and R321 and Tub2p residues R62, D67, E123, E128, D203, and R318.

The distribution of mutations in different phenotypic classes was examined. Tubulin mutations often result in the unusual phenotype of cold sensitivity. As shown in Figure 5, the distribution of the cold-sensitive alleles is striking; all these alleles, in both Tub1p and Tub2p, lie either at or near the lateral contacts between protofilaments or in longitudinal contacts between tubulin monomers along the protofilament. In other words, virtually every cold-sensitive tubulin Ala-scan mutation is physically in a position to disrupt the polymerized microtubule structure by altering tubulin-tu-

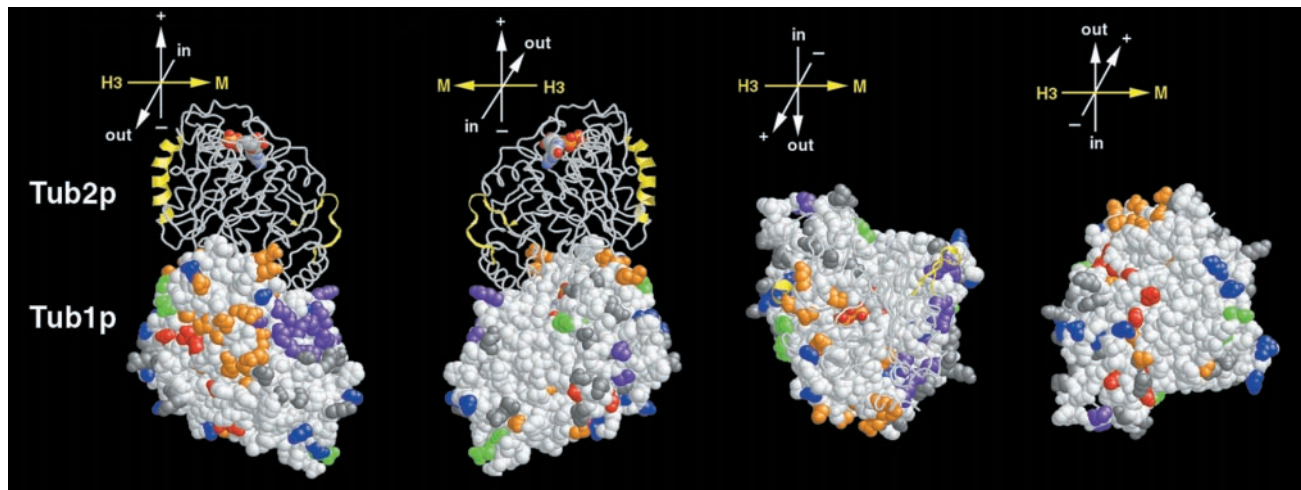


**Figure 4.** Distribution of alanine-scanning mutations in Tub1p. Side chains of amino acids altered by *tub1* mutations are colored as in Figure 1: Green, wild-type; red, lethal; blue, cold-sensitive; orange, slow growth; gray, benomyl-supersensitive; purple, benomyl-resistant. Tub2p shown as a backbone trace, and Tub1p is shown as space-filled atoms. Lateral interaction elements,  $\alpha$ -helix H3 and M loop, are shown in yellow in Tub2p (Nogales *et al.*, 1999). Orientation axes: + and - show microtubule orientation; H3 and M show lateral sides marked by helix H3  $\alpha$ -helix and M loop, respectively; in and out represent the inside and the outside of the microtubule, respectively. Structure drawn using RASMOL (Sayle and Milner-White, 1995).

bulin contacts. This is consistent with the fact that microtubules are known to be cold-sensitive structures.

The mutations producing a benomyl-resistant phenotype were mapped onto the tubulin model. Benomyl-resistant mutations were split into two classes; five *tub2* mutants were resistant to very high concentrations of benomyl (75 or 80  $\mu\text{g/ml}$ ), and the remainder were resistant only to lesser concentrations. In wild-type Tub2p each of the five (Figure 6, orange) contain component charged residues (123, 197, 198, and 318) in a pocket relatively deep in the tubulin structure (unusual for charged residues). This pocket, situated between the  $\beta$ -sheet S1-S6, helix H8 and the core helix H7, is also the site of several other highly benomyl-resistant mutations, *tub2-201* (L253V), *tub2-104* (R241H), and the benomyl-dependent *tub2-150* (T238A) (Figure 6, purple; Thomas, 1984; Thomas *et al.*, 1985; Machin *et al.*, 1995). It seems possible, although we have no more direct evidence, that this pocket might be associated with either benomyl binding or a conformational response to benomyl binding. Consistent with this possibility, residue 198 is found to be changed in many benomyl-resistant mutations in the  $\beta$ -tubulin-encoding genes of a variety of species other than *S. cerevisiae* (e.g., Fujimura *et al.*, 1992; Jung *et al.*, 1992; Buhr and Dickman, 1994; Park *et al.*, 1997).

The second class of benomyl-resistant alleles includes both *tub1* and *tub2* alleles. Whereas these benomyl-resistant *tub2* mutations are distributed across Tub2p, all of the benomyl-resistant *tub1* alleles except one cluster to a face of Tub1p near the lateral protofilament contact but exposed to the outer surface of the microtubule. Because an increased level of  $\alpha$ -tubulin can cause benomyl resistance (Schatz *et al.*, 1986b), it is a formal possibility that these mutations might increase the quantity of functional  $\alpha$ -tubulin. Alternatively, they might disrupt the binding of a protein that acts to destabilize microtubules. For example, deletion of the *DYN1*

or *KIP1* genes encoding microtubule motor proteins results in benomyl resistance and increased microtubule length (Cottingham and Hoyt, 1997). Interestingly, several benomyl-resistant mutations in both *tub1* and *tub2* map to loops that would be in the interior of an assembled microtubule (Figure 6, see *tub1-806* and *tub2-410* and *-411*).

### Residues Affecting Bim1p Binding

We previously described a microtubule-binding protein, Bim1p, and demonstrated that it bound to Tub1p in the two-hybrid system and decorated microtubules *in vivo*. All of the *tub1* Ala-scan alleles were tested for binding to Bim1p in the two-hybrid system, and *tub1* mutations that disrupted binding were found to cluster at the C terminus of Tub1p (Schwartz *et al.*, 1997). The *tub1* mutations that disrupt Bim1p binding are mapped on the structure of  $\alpha$ -tubulin in Figure 7. Most of these mutations cluster in a region facing outward in the assembled microtubule; however, there are several (*tub1-809*, *-813*, *-842*, and *-846*) that were located at the intradimer interface. Perhaps an  $\alpha$ - $\beta$  dimer must be formed to achieve a positive two-hybrid interaction with Bim1p. Two-hybrid interactions were not tested between Bim1p and the Tub2p Ala-scan mutants, because the ectopic expression of Tub2p from these plasmids was lethal, as expected (Burke *et al.*, 1989; Weinstein and Solomon, 1990).

A similar approach has been used to delineate the interaction footprint of another Tub1p-binding protein, Alf1p (Feierbach *et al.*, 1999), which lies at a site overlapping but not identical to the Bim1p footprint at the C terminus of Tub1p, on the outside face of the microtubule. Motor proteins, such as dynein and kinesin, have also been shown to bind  $\beta$ -tubulin, also at the C terminus (Goldsmith *et al.*, 1995; Hirose *et al.*, 1995; Hoenger *et al.*, 1995).

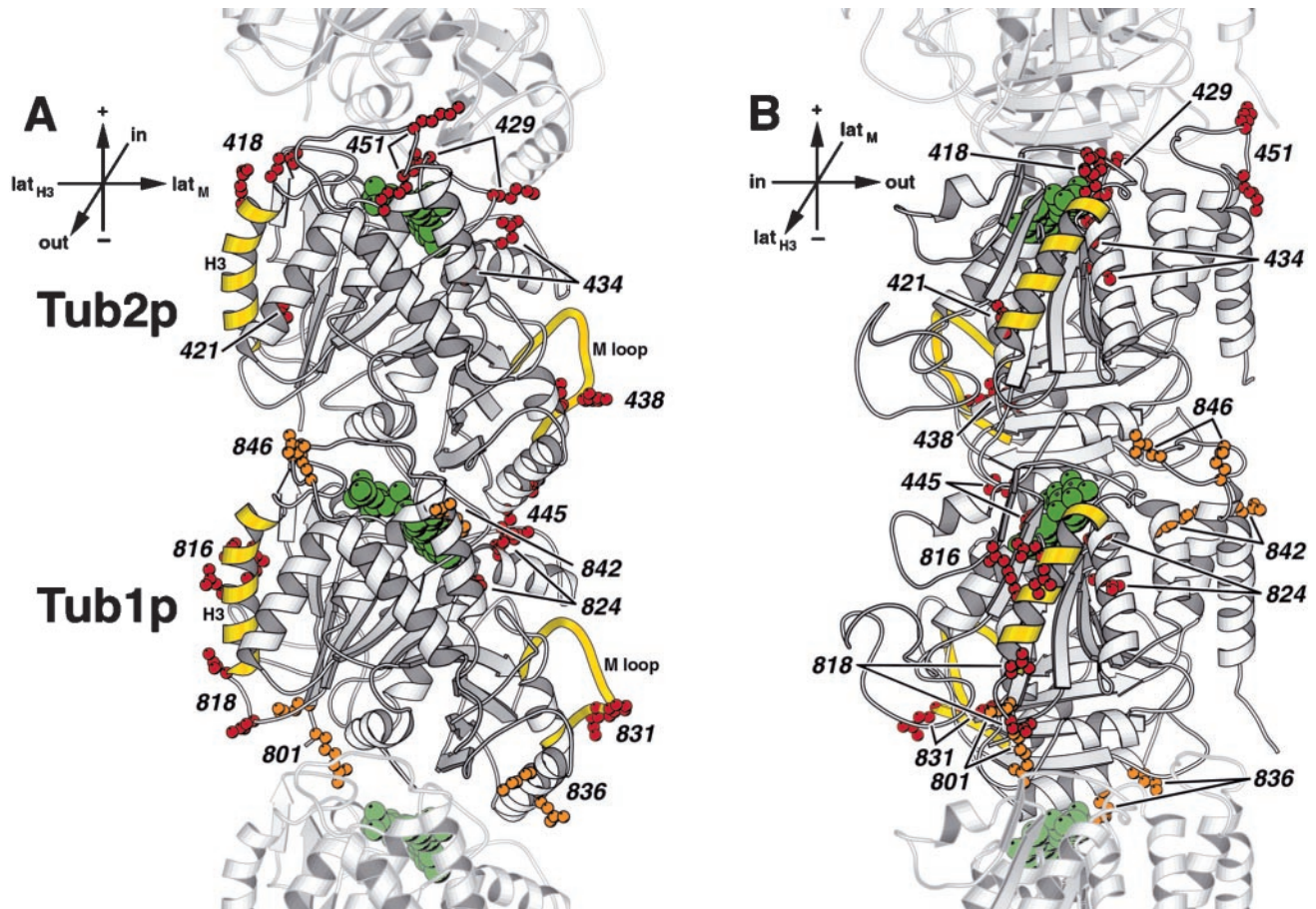


**Figure 5.** Mutations resulting in cold sensitivity are located in areas of the tubulin protein involved in longitudinal or lateral contacts in the microtubule polymer. (A) View from the outside of the microtubule. (B) View from the side of the protofilament. The side chains of amino acids mutated in cold-sensitive alleles (red) and temperature- and cold-sensitive alleles (orange) are shown on Tub2p (top) and Tub1p (bottom) of the yeast tubulin heterodimer. These amino acids are labeled by their allele number. Lateral interaction elements,  $\alpha$ -helix H3 and M-loop, are shown in yellow (Nogales *et al.*, 1999). GTP and GDP are shown in green. Adjacent monomers of the protofilament are shown in lighter gray. Orientation axes: + and - show microtubule orientation; lat<sub>H3</sub> and lat<sub>M</sub> show lateral sides marked by helix H3 and M loop, respectively; in and out represent the inside and the outside of the microtubule, respectively. Structure drawn using MOLSCRIPT (Kraulis, 1991).

### Double Mutant Analysis

Another approach to examine interactions between two proteins is by differential genetic interactions. We tested the genetic interactions between each of the *tub1* Ala-scan mutants and a benomyl-resistant mutant, *tub2-201*. The *tub2-201* mutation confers a high level of benomyl resistance but no other discernible phenotypes (Thomas, 1984). When sequenced, *tub2-201* contained a Leu to Val change at position 253, which maps to the interior side of helix H8 at the intradimer interface (see Figures 6 and 8). DBY7830, which contains *tub2-201* back-crossed into the DBY6654 strain background (Schwartz *et al.*, 1997), was crossed to each of the *tub1* Ala-scan mutants. The double mutants displayed a range of phenotypes, from wild-type growth to synthetic lethality. On media containing benomyl, the double mutants generally showed additive effects; i.e., they displayed the benomyl resistance of *tub2-201*; but somewhat diminished commensurate with the degree of

benomyl sensitivity of the single *tub1* mutant. The *tub1* mutations that were synthetically lethal in combination with *tub2-201* are shown in Figure 8. These *tub1* alleles (-809, -813, -814, -845, and -853) cluster at the intradimer interface. This suggests that *tub2-201*, although nearly wild-type in phenotype, may cause a distortion of its intradimer interface. When *tub2-201* is combined with *tub1* mutations at the intradimer interface, the  $\alpha$ - $\beta$  dimer interaction may become so unstable as to cause death. In support of this hypothesis, *tub1-814* contains a mutant residue 106 that is known to be important for stabilizing the intradimer interaction in yeast (Vega *et al.*, 1998).

### Conclusion

The *TUB1* mutations described here complete the systematic mutagenesis of the genes encoding the major subunits of the yeast cytoskeleton. Although there are two  $\alpha$ -tubulin-encod-

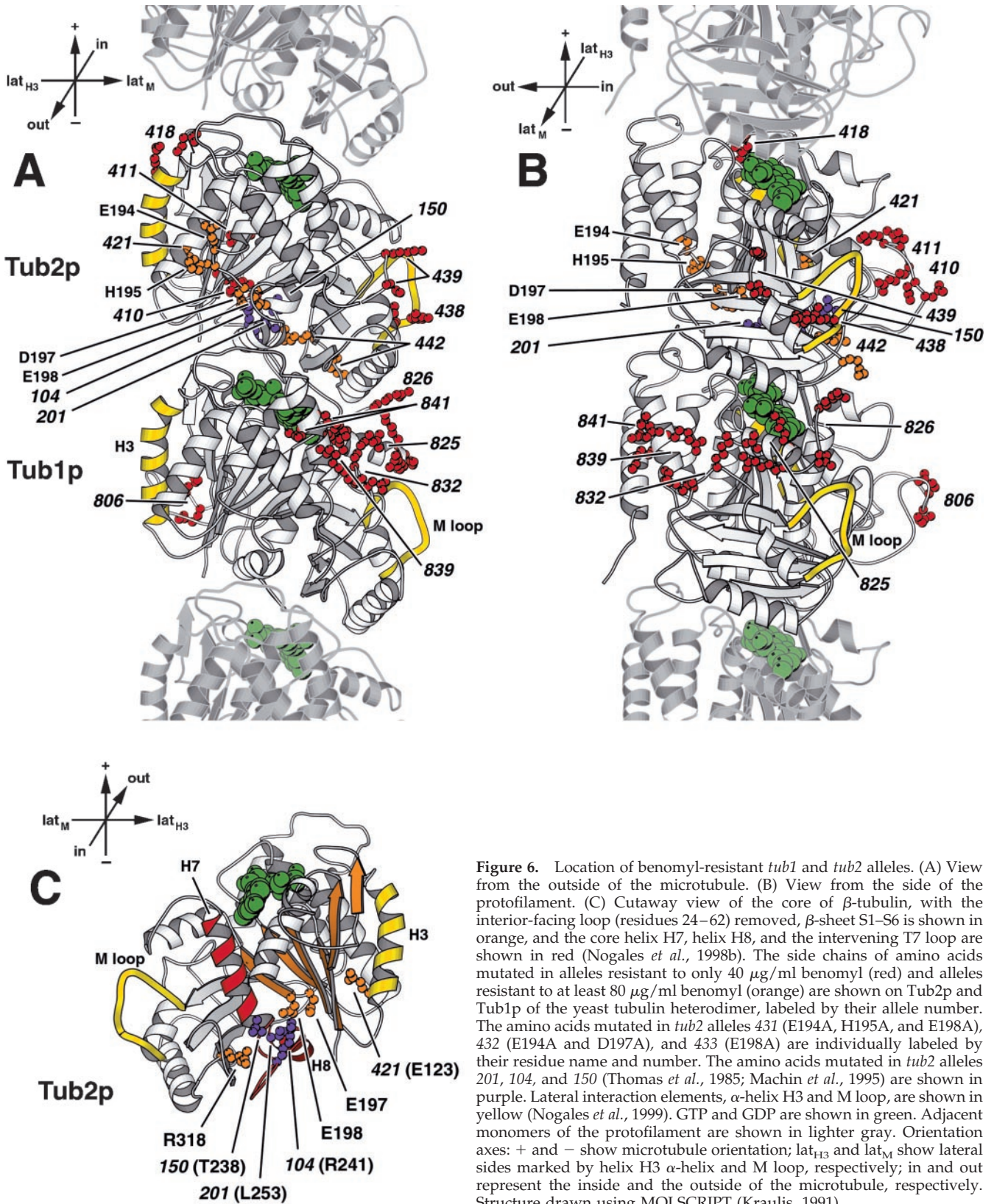


**Figure 6.** Location of benomyl-resistant *tub1* and *tub2* alleles. (A) View from the outside of the microtubule. (B) View from the side of the protofilament. (C) Cutaway view of the core of β-tubulin, with the interior-facing loop (residues 24–62) removed, β-sheet S1–S6 is shown in orange, and the core helix H7, helix H8, and the intervening T7 loop are shown in red (Nogales *et al.*, 1998b). The side chains of amino acids mutated in alleles resistant to only 40 μg/ml benomyl (red) and alleles resistant to at least 80 μg/ml benomyl (orange) are shown on Tub2p and Tub1p of the yeast tubulin heterodimer, labeled by their allele number. The amino acids mutated in *tub2* alleles 431 (E194A, H195A, and E198A), 432 (E194A and D197A), and 433 (E198A) are individually labeled by their residue name and number. The amino acids mutated in *tub2* alleles 201, 104, and 150 (Thomas *et al.*, 1985; Machin *et al.*, 1995) are shown in purple. Lateral interaction elements, α-helix H3 and M loop, are shown in yellow (Nogales *et al.*, 1999). GTP and GDP are shown in green. Adjacent monomers of the protofilament are shown in lighter gray. Orientation axes: + and – show microtubule orientation; lat<sub>H3</sub> and lat<sub>M</sub> show lateral sides marked by helix H3 α-helix and M loop, respectively; in and out represent the inside and the outside of the microtubule, respectively. Structure drawn using MOLSCRIPT (Kraulis, 1991).

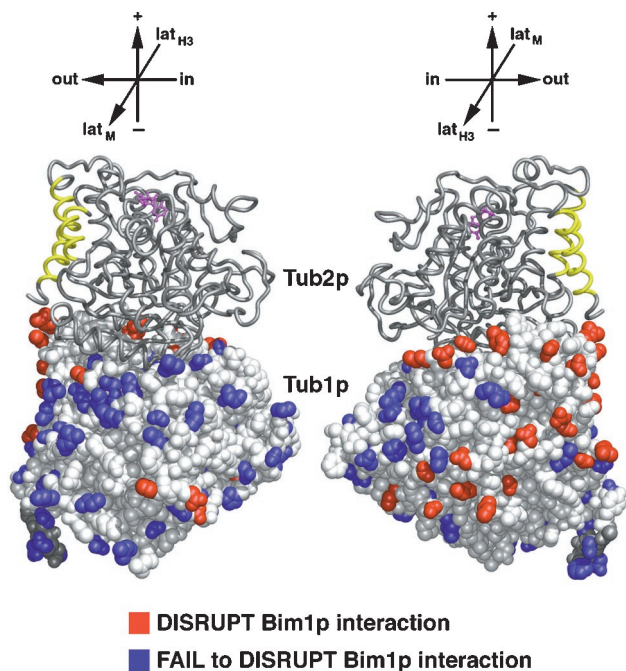


**Figure 7.** Two-hybrid interaction footprint of Bim1p on Tub1p. Bim1p was tested for interaction with each of the Tub1p mutant proteins using the two-hybrid system. Those *tub1* mutations that abolished the two-hybrid interaction are shown in red; those *tub1* mutations that still interacted are shown in blue (Schwartz *et al.*, 1997). Structure drawn using MIDAS (Ferrin *et al.*, 1988).

ing genes, *TUB1* and *TUB3* are so similar that it is likely that it will be possible to study virtually all structure–function relationships with associated proteins using the mutations already in hand. Mapping of the mutations to the surface will provide, for tubulin, genetic tools for structure–function analysis analogous to those that have served so well in the case of actin, in which mutations derived from a similar systematic mutagenesis scheme have served to connect residues on the actin three-dimensional structure to binding regions for a great variety of ligands. To illustrate this, the new *tub1* mutants described here have allowed us to understand better the interaction of  $\alpha$ - with  $\beta$ -tubulin and  $\alpha$ -tubulin with Bim1p and to suggest the location of the benomyl-binding site by placing *tub2* mutations on the structure.

## ACKNOWLEDGMENTS

We thank Charles Scafe for assistance with molecular modeling and Tim Stearns and Becket Feierbach for helpful discussions. This work was supported by a grant from the National Institutes of Health (GM-46406) to D.B. and a National Institutes of Health Postdoctoral Fellowship to K.R.A.

## REFERENCES

- Amberg, D.C., Basart, E., and Botstein, D. (1995). Defining protein interactions with yeast actin *in vivo*. *Nat. Struct. Biol.* 2, 28–35.
- Arce, C.A., Hallak, M.E., Rodriguez, J.A., Barra, H.S., and Caputto, R. (1978). Capability of tubulin and microtubules to incorporate and

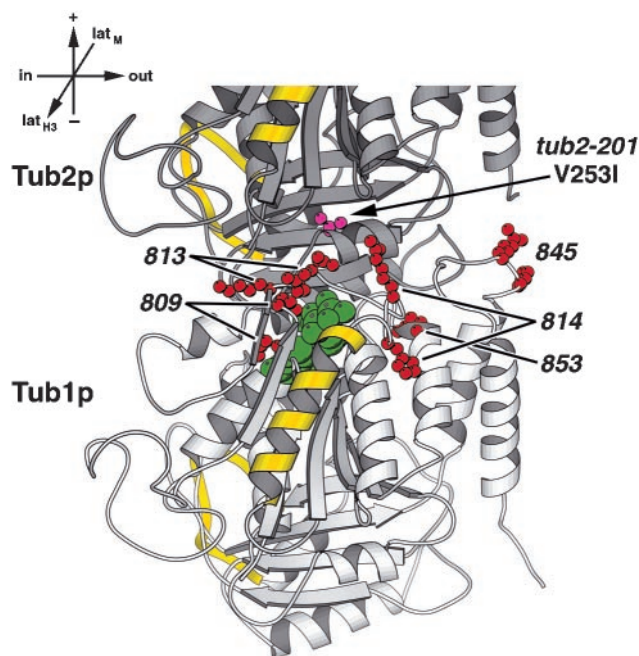


**Figure 8.** *tub1* alleles that are synthetically lethal with *tub2-201* localize to the intradimer interface. Amino acids mutated in these *tub1* alleles (red) are shown on Tub1p (bottom). Tub2p is partly shown above with the *tub2-201* mutant residue shown in magenta. Lateral interaction elements,  $\alpha$ -helix H3 and M loop, are shown in yellow (Nogales *et al.*, 1999). GTP is shown in green. The view is from the side of the heterodimer. Orientation axes: + and – show microtubule orientation;  $lat_{H3}$  and  $lat_M$  show lateral sides marked by helix H3 and M loop, respectively; in and out represent the inside and the outside of the microtubule, respectively. Structure drawn using MOLSCRIPT (Kraulis, 1991).

to release tyrosine and phenylalanine and the effect of the incorporation of these amino acids on tubulin assembly. *J. Neurochem.* 31, 205–210.

- Argarana, C.E., Barra, H.S., and Caputto, R. (1978). Release of [<sup>14</sup>C]tyrosine from tubulinyl-[<sup>14</sup>C]tyrosine by brain extract. Separation of a carboxypeptidase from tubulin-tyrosine ligase. *Mol. Cell. Biochem.* 19, 17–21.
- Bai, C., and Elledge, S.J. (1996). Gene identification using the yeast two-hybrid system. *Methods Enzymol.* 273, 331–347.
- Bairoch, A. (1991). PROSITE: a dictionary of sites and patterns in proteins. *Nucleic Acids Res.* 19, 2241–2246.
- Barra, H.S., Arce, C.A., and Argarana, C.E. (1988). Posttranslational tyrosination/detyrosination of tubulin. *Mol. Neurobiol.* 2, 133–153.
- Bass, S.H., Mulkerrin, M.G., and Wells, J.A. (1991). A systematic mutational analysis of hormone-binding determinants in the human growth hormone receptor. *Proc. Natl. Acad. Sci. USA* 88, 4498–4502.
- Becker, D.M., and Guarente, L. (1991). High-efficiency transformation of yeast by electroporation. In: *Methods in Enzymology, Guide to Yeast Genetics and Molecular Biology*, vol. 194, ed. C. Guthrie and G.R. Fink, San Diego: Academic Press, 182–187.
- Bennett, W.F., Paoni, N.F., Keyt, B.A., Botstein, D., Jones, A.J.S., Presta, L., Wurm, F.M., and Zoller, M.J. (1991). High resolution analysis of functional determinants on human tissue-type plasminogen activator. *J. Biol. Chem.* 266, 5191–5201.

- Bowman, S., *et al.* (1997). The nucleotide sequence of *Saccharomyces cerevisiae* chromosome XIII. *Nature* 387, 90–93.
- Buhr, T.L., and Dickman, M.B. (1994). Isolation, characterization, and expression of a second beta-tubulin-encoding gene from *Colletotrichum gloeosporioides* f. sp. *aeschyromene*. *Appl. Environ. Microbiol.* 60, 4155–4159.
- Burke, D., Gasdaska, P., and Hartwell, L. (1989). Dominant effects of tubulin overexpression in *Saccharomyces cerevisiae*. *Mol. Cell. Biol.* 9, 1049–1059.
- Burns, R.G. (1991). Alpha-, beta-, and gamma-tubulins: sequence comparisons and structural constraints. *Cell Motil. Cytoskeleton* 20, 181–189.
- Cali, B.M., Doyle, T.C., Botstein, D., and Fink, G.R. (1998). Multiple functions for actin during filamentous growth of *Saccharomyces cerevisiae*. *Mol. Biol. Cell* 9, 1873–1889.
- Cleveland, D.W., Joshi, H.C., and Murphy, D.B. (1990). Tubulin site interpretation. *Nature* 344, 389.
- Cottingham, F.R., and Hoyt, M.A. (1997). Mitotic spindle positioning in *Saccharomyces cerevisiae* is accomplished by antagonistically acting microtubule motor proteins. *J. Cell Biol.* 138, 1041–1053.
- Feierbach, B., Nogales, E., Downing, K.H., and Stearns, T. (1999). Alf1p, a CLIP-170 domain-containing protein, is functionally and physically associated with alpha-tubulin. *J. Cell Biol.* 144, 113–124.
- Ferrin, T.E., Huang, C.C., Jarvis, L.E., and Langridge, R. (1988). The MIDAS Display System. *J. Mol. Graph* 6, 13–37.
- Fujimura, M., Oeda, K., Inoue, H., and Kato, T. (1992). A single amino-acid substitution in the beta-tubulin gene of *Neurospora* confers both carbendazim resistance and diethofencarb sensitivity. *Curr. Genet.* 21, 399–404.
- Gibbs, C.S., and Zoller, M.J. (1991). Rational scanning mutagenesis of a protein kinase identifies functional regions involved in catalysis and substrate interactions. *J. Biol. Chem* 266, 8923–8931.
- Goldsmith, M., Yarbrough, L., and van der Kooy, D. (1995). Mechanics of motility: distinct dynein binding domains on alpha- and beta-tubulin. *Biochem. Cell Biol.* 73, 665–671.
- Guex, N., and Peitsch, M.C. (1997). SWISS-MODEL and the Swiss-PdbViewer: an environment for comparative protein modeling. *Electrophoresis* 18, 2714–2723.
- Hirose, K., Lockhart, A., Cross, R.A., and Amos, L.A. (1995). Nucleotide-dependent angular change in kinesin motor domain bound to tubulin. *Nature* 376, 277–279.
- Hoenger, A., Sablin, E.P., Vale, R.D., Fletterick, R.J., and Milligan, R.A. (1995). Three-dimensional structure of a tubulin-motor-protein complex. *Nature* 376, 271–274.
- Huffaker, T.C., Thomas, J.H., and Botstein, D. (1988). Diverse effects of beta-tubulin mutations on microtubule formation and function. *J. Cell Biol.* 106, 1997–2010.
- Huh, W.K., Lee, B.H., Kim, S.T., Kim, Y.R., Rhie, G.E., Baek, Y.W., Hwang, C.S., Lee, J.S., and Kang, S.O. (1998). D-Erythroascorbic acid is an important antioxidant molecule in *Saccharomyces cerevisiae*. *Mol. Microbiol.* 30, 895–903.
- Hyams, J.S., and Lloyd, C.W. (1994). Microtubules. In: *Modern Cell Biology*, vol. 13, J.B. Harford (ed.), New York: Wiley-Liss.
- Jacobs, C.W., Adams, A.E., Szaniszlo, P.J., and Pringle, J.R. (1988). Functions of microtubules in the *Saccharomyces cerevisiae* cell cycle. *J. Cell Biol.* 107, 1409–1426.
- Jones, J.S., and Prakash, L. (1990). Yeast *Saccharomyces cerevisiae* selectable markers in pUC18 polylinkers. *Yeast* 6, 363–366.
- Jung, M.K., Wilder, I.B., and Oakley, B.R. (1992). Amino acid alterations in the *benA* (beta-tubulin) gene of *Aspergillus nidulans* that confer benomyl resistance. *Cell Motil. Cytoskeleton* 22, 170–174.
- Kassir, Y., and Simchen, G. (1991). Monitoring meiosis and sporulation in *Saccharomyces cerevisiae*. *Methods Enzymol.* 194, 94–110.
- Kraulis, P.J. (1991). MOLSCRIPT: a program to produce both detailed and schematic plots of protein structures. *J. Appl. Crystallogr.* 24, 946–950.
- Kunkel, T.A., Roberts, J.D., and Zakour, R.A. (1987). Rapid and efficient site-specific mutagenesis without phenotypic selection. *Methods Enzymol.* 154, 367–382.
- Lappalainen, P., Fedorov, E.V., Fedorov, A.A., Almo, S.C., and Drubin, D.G. (1997). Essential functions and actin-binding surfaces of yeast cofilin revealed by systematic mutagenesis. *EMBO J.* 16, 5520–5530.
- Little, M., and Seehaus, T. (1988). Comparative analysis of tubulin sequences. *Comp. Biochem. Physiol.* 90, 655–670.
- Machin, N.A., Lee, J.M., and Barnes, G. (1995). Microtubule stability in budding yeast: characterization and dosage suppression of a benomyl-dependent tubulin mutant. *Mol. Biol. Cell* 6, 1241–1259.
- Miller, C.J., Doyle, T.C., Bobkova, E., Botstein, D., and Reisler, E. (1996). Mutational analysis of the role of hydrophobic residues in the 338–348 helix on actin in actomyosin interactions. *Biochemistry* 35, 3670–3676.
- Neff, N.F., Thomas, J.H., Grisafi, P., and Botstein, D. (1983). Isolation of the beta-tubulin gene from yeast and demonstration of its essential function *in vivo*. *Cell* 33, 211–219.
- Nogales, E., Downing, K.H., Amos, L.A., and Lowe, J. (1998a). Tubulin and FtsZ form a distinct family of GTPases. *Nat. Struct. Biol.* 5, 451–458.
- Nogales, E., Whittaker, M., Milligan, R.A., and Downing, K.H. (1999). High-resolution model of the microtubule. *Cell* 96, 79–88.
- Nogales, E., Wolf, S.G., and Downing, K.H. (1998b). Structure of the alpha beta tubulin dimer by electron crystallography. *Nature* 391, 199–203.
- Park, S.Y., Jung, O.J., Chung, Y.R., and Lee, C.W. (1997). Isolation and characterization of a benomyl-resistant form of beta-tubulin-encoding gene from the phytopathogenic fungus *Botryotinia fuckeliana*. *Mol. Cells* 7, 104–109.
- Pasqualone, D., and Huffaker, T.C. (1994). *STU1*, a suppressor of a beta-tubulin mutation, encodes a novel and essential component of the yeast mitotic spindle. *J. Cell Biol.* 127, 1973–1984.
- Reijo, R.A., Cooper, E.M., Beagle, G.J., and Huffaker, T.C. (1994). Systematic mutational analysis of the yeast beta-tubulin gene. *Mol. Biol. Cell* 5, 29–43.
- Rose, M.D., Winston, F., and Hieter, P. (1990). *Methods in Yeast Genetics: A Laboratory Course Manual*, Cold Spring Harbor, NY: Cold Spring Harbor Laboratory Press.
- Sambrook, J., Fritsch, E.F., and Maniatis, T. (1989). *Molecular Cloning: A Laboratory Manual*, Cold Spring Harbor, NY: Cold Spring Harbor Laboratory Press.
- Sayle, R.A., and Milner-White, E.J. (1995). RASMOL: biomolecular graphics for all. *Trends Biochem. Sci.* 20, 374.
- Schatz, P.J., Pillus, L., Grisafi, P., Solomon, F., and Botstein, D. (1986a). Two functional alpha-tubulin genes of the yeast *Saccharomyces cerevisiae* encode divergent proteins. *Mol. Cell. Biol.* 6, 3711–3721.
- Schatz, P.J., Solomon, F., and Botstein, D. (1986b). Genetically essential and nonessential alpha-tubulin genes specify functionally interchangeable proteins. *Mol. Cell. Biol.* 6, 3722–3733.

- Schatz, P.J., Solomon, F., and Botstein, D. (1988). Isolation and characterization of conditional-lethal mutations in the *TUB1* alpha-tubulin gene of the yeast *Saccharomyces cerevisiae*. *Genetics* 120, 681–695.
- Schwartz, K., Richards, K., and Botstein, D. (1997). *BIM1* encodes a microtubule-binding protein in yeast. *Mol. Biol. Cell* 8, 2677–2691.
- Sherman, G., Rosenberry, T.L., and Sternlicht, H. (1983). Identification of lysine residues essential for microtubule assembly. Demonstration of enhanced reactivity during reductive methylation. *J. Biol. Chem.* 258, 2148–2156.
- Sikorski, R.S., and Hieter, P. (1989). A system of shuttle vectors and yeast host strains designed for efficient manipulation of DNA in *Saccharomyces cerevisiae*. *Genetics* 122, 19–27.
- Szasz, J., Yaffe, M.B., Elzinga, M., Blank, G.S., and Sternlicht, H. (1986). Microtubule assembly is dependent on a cluster of basic residues in alpha-tubulin. *Biochemistry* 25, 4572–4582.
- Thomas, J.H. (1984). Genes Controlling the Mitotic Spindle and Chromosome Segregation in Yeast. Ph.D. Thesis. Cambridge, MA: Massachusetts Institute of Technology.
- Thomas, J.H., Neff, N.F., and Botstein, D. (1985). Isolation and characterization of mutations in the beta-tubulin gene of *Saccharomyces cerevisiae*. *Genetics* 111, 715–734.
- Vega, L.R., Fleming, J., and Solomon, F. (1998). An alpha-tubulin mutant destabilizes the heterodimer: phenotypic consequences and interactions with tubulin-binding proteins. *Mol. Biol. Cell* 9, 2349–2360.
- Weinstein, B., and Solomon, F. (1990). Phenotypic consequences of tubulin overproduction in *Saccharomyces cerevisiae*: differences between alpha-tubulin and beta-tubulin. *Mol. Cell. Biol.* 10, 5295–5304.
- Wertman, K.F., Drubin, D.G., and Botstein, D. (1992). Systematic mutational analysis of the yeast *ACT1* gene. *Genetics* 132, 337–350.